BRAF mutation and *CDKN2A* deletion define a clinically distinct subgroup of childhood secondary high-grade glioma

by

Matthew R. Mistry

A thesis submitted in conformity with the requirements
for the degree of Masters of Science

Institute of Medical Science
University of Toronto

BRAF mutation and *CDKN2A* deletion define a clinically distinct subgroup of childhood secondary high-grade glioma

Matthew R. Mistry

Masters of Science

Institute of Medical Science
University of Toronto

2014

Abstract

This thesis sought to uncover genetic events leading to transformation of pediatric low-grade glioma (PLGG) to secondary high-grade glioma (sHGG) and to define transformation risk using a population-based cohort (n=888) of PLGG with long clinical follow-up. We hypothesize early somatic exonic alterations, which are poorly understood, contribute to transformation. sHGG were observed in 3.2% of patients. *BRAF* and *CDKN2A* alterations were observed in 39% and 57% of sHGG respectively. All *BRAF* and 80% of *CDKN2A* alterations could be traced back to patient-matched PLGG counterparts. BRAF V600E distinguished secondary from primary HGG ($p=0.0023$), while *BRAF* and *CDKN2A* alterations were rarely observed in non-transformed PLGG ($p<0.0001$ and $p=0.0007$ respectively). The *BRAF*-mutant subgroup had longer latency periods than wildtype-*BRAF* PLGG (6.65 versus 1.60 years; $p=0.0389$). Five-year overall survival of children with *BRAF*-mutant and wildtype-PLGG that transformed were 75%±15% and 29%±12%, respectively ($p=0.024$). *BRAF* mutations constitute a molecular and clinically distinct subtype of sHGG.

Acknowledgments

There are numerous people who have shaped my personal and professional growth during my graduate training over the past few years. First and foremost, my supervisor, Dr. Uri Tabori, has been an inspirational mentor and advisor who I am incredibly fortunate to be learning from. I sincerely thank him for his patience and providing uncountable hours of mentorship, numerous opportunities for my professional development and a challenging academic training environment, all of which have made me a better researcher and motivated me to continuously follow my passions.

I also need to thank the members of my program advisory committee, Dr. Cynthia Hawkins and Dr. Annie Huang, for their genuine interest in and support for my research project. I am particularly appreciative to Dr. Hawkins for always offering her invaluable expertise and the enormous amount of time she invested in advising me, both professionally and personally.

I would like to thank Daniele Merico, Sergio Pereira and the informatics team at The Center for Applied Genomics at SickKids, for their efforts to this project. I also want to thank Jim Stavropoulos, Mary Shago, Peter Ray and their staff from the Division of Molecular Genetics, Department of Pediatric Laboratory Medicine, SickKids, for their contributions.

I would like to say a tremendous thank you to our lab manager, Cindy Zhang, for being an invaluable resource during the entirety of my academic training.

I also want to thank Dr. David Malkin for his mentorship and expertise during my research training. I also thank his laboratory technician, Noa Alon, who was always more than willing to troubleshoot an experiment with me.

A genuine thank you to the past and present members of the Tabori, Hawkins and Malkin labs, and the Brain Tumor Research Center at SickKids, for their technical support to my project, but also their humor and friendship, which thoroughly enriched my graduate student experience.

Finally, I am very thankful to have exceptionally supportive friends who continued to encourage me despite the many setbacks and difficulties I encountered during my graduate training. Most of all, I am grateful to my parents who have always been a source of comfort and calm to me. Their unwavering belief in my abilities gives me the confidence to continue challenging myself academically, and whose numerous sacrifices motivate me to keep reaching for my professional aspirations.

Data attribution

This thesis consists of two parts: biological and clinical data. This work represents an extensive collaborative effort on the behalf of a number of individuals.

For the clinical part of the thesis, cohort assembly, statistical analysis and interpretation of the results were performed by Matthew Mistry. Clinical data collection was performed by Matthew Mistry, Nataliya Zhukova, Rahul Krishnatry, and Doua Bakry. Clinical and biological data on individual patients used in this study were provided by Dr. Uri Tabori and Dr. Cynthia Hawkins, The Hospital for Sick Children, Toronto Ontario, Canada; Dr. Keith Ligon, Dana Farber Cancer Center, Boston, U.S.A; Jennifer Chan, Hotchkiss Brain Institute, University of Calgary, Alberta, Canada.

Conceptualization of the thesis, experimental design and execution of biological experiences, data analysis and interpretations were performed by Matthew Mistry. A portion of the whole-exome sequencing somatic variant analysis was performed by Daniele Merico, TCAG, and Adam Shlien, SickKids. Vilma Navickiene, DPLM, aided in cast-PCR experiments. Immunohistochemistry and interphase FISH experiments were performed at the Pathology Research Program (PRP) at the University Health Network and DPLM at SickKids.

Table of Contents

1 Table of Contents

List of Abbreviations

ATRX	Alpha thalassemia/mental retardation syndrome X-linked
ALT	Alternative lengthening of telomeres
AA	Anaplastic astrocytoma
AG	Anaplastic ganglioglioma
APXA	Anaplastic pleomorphic xanthoastrocytoma
BRAF	v-raf murine sarcoma viral oncogene homolog B
bMMRD	Biallelic mismatch repair deficiency syndrome
CNS	Central nervous system
CDK4	Cyclin-dependent kinase 4
CDK6	Cyclin-dependent kinase 6
CDKN2A	Cyclin-dependent kinase inhibitor 2A
CCND1	Cyclin-D1
DAXX	death-domain associated protein
DPLM	Department of Pathology and Laboratory Medicine
DIPG	Diffuse intrinsic pontine glioma
EGFR	Epidermal growth factor receptor
ERK	Extra-cellular signal regulated kinases
ETS	E26 transformation-specific

FGFR1	Fibroblast growth factor receptor 1
GG	Ganglioglioma
GBM	Glioblastoma multiforme
G1	Growth phase 1
GTP	Guanosine-5'-triphosphate
H3F3A	H3 Histone, Family 3A
hTERT	Human telomerase reverse transcriptase
HPM	Hypermutator phenotype
IDH1	isocitrate dehydrogenase 1
IDH2	isocitrate dehydrogenase 2
KIAA1549	KIAA1549
LFS	Li-Fraumeni syndrome
LGA	Low grade astrocytoma
MT	Malignant transformation
Mb	Megabase
MAPK	Mitogen-activated protein kinases
MYB	v-myb avian myeloblastosis viral oncogene homolog
MYBL1	v-myb avian myeloblastosis viral oncogene homolog-like 1
NF1	Neurofibromin 1
OIS	Oncogene induced senescence

OS	Overall survival
PLGG	Pediatric low grade glioma
PTEN	Phosphatase and tensin homolog
PIK3CA	Phosphatidylinositol-4,5-bisphosphate 3-kinase, catalytic subunit alpha
PA	Pilocytic astrocytoma
PDGFRA	Platelet-derived growth factor receptor, alpha polypeptide
PXA	Pleomorphic xanthoastrocytoma
PMS2	PMS2 postmeiotic segregation increased 2 (S. cerevisiae)
pHGG	Primary high grade glioma (pediatric)
PFS	Progression-free survival
RAF1	V-raf-1 murine leukemia viral oncogene homolog
RT	Radiotherapy
RB1	Retinoblastoma 1
sHGG	Secondary high grade glioma
S	Synthesis phase
TCAG	The Center for Applied Genomics
TF	Transcription factor
TP53	Tumor protein p53
UHN	University Health Network
WHO	World Health Organization

List of Tables

CHAPTER 3: RESULTS

List of Figures

CHAPTER 2: METHODS AND MATERIALS

CHAPTER 3: RESULTS

CHAPTER 4: DISCUSSION

List of Appendices

1 CHAPTER 1: INTRODUCTION

My thesis revolves around the finding of molecular and genetic alterations which are causing malignant transformation of childhood low-grade glioma to high grade tumors. This is the single most common cause of death of these children. I chose to use next-generation sequencing tools to uncover alterations responsible for this devastating process. In order to put this thesis in context, a brief introduction is warranted.

Gliomas are the most common central nervous system neoplasm in children. The term glioma refers to tumors arising from cells of the glial lineage, which are similar to astrocytes, ependymal cells and oligodendrocytes. Glioma is a heterogeneous group of tumors that are classified by morphology, cell type and histological features according to the World Health Organization (WHO) grading criteria. The WHO classification uses this histological grading system to predict biological behavior. Children diagnosed with glioma have a wide range of clinical outcomes, ranging from very long overall survival to very short, depending on the grade assigned and clinical presentation of the tumor. Pediatric low-grade gliomas (PLGG) have excellent long term survival partially due to the fact that transformation to high-grade tumors is rare in childhood PLGG. Due to its rarity, and lack of the appropriate tools used on this cohort, the events leading to transformation of PLGG are largely unknown.

In contrast, adult low-grade glioma invariantly transform to high grade tumors. Indeed, the evolution of adult high-grade glioma is well studied in comparison to the childhood disease-counterpart. In adults, there are two types of high-grade glioma, termed primary and secondary high-grade glioma, the latter of which develops progressively from lower-grade lesions. Childhood “secondary high grade gliomas” is an unknown entity which I will try to explore. A

review of the current literature outlining the clinical and molecular differences between these two types of adult high-grade glioma will be reviewed first as this thesis serves to investigate the genetic evolution of secondary high-grade glioma in children, which has yet to be described. Moreover, this thesis investigates genetic and molecular alterations that define secondary HGG in children, and seeks to determine which events occur early in the transformation of low-grade tumors to high-grade glioma. This thesis will begin by describing the specific genetic and molecular alterations that distinguish primary from secondary HGG in adults to give appropriate background when considering what is known about glioma transformation in the pediatric setting.

1.1 Adult High-Grade Glioma

1.1.1 Clinical characteristics and outcome

Glioma refers to those tumors arising from astrocytic and oligodendroglioma lineages, however, only features of the astrocytic lineage will be described. The most frequent and aggressive primary malignant brain tumor in adults is glioblastoma multiforme (GBM), which remains virtually incurable. The WHO categorizes GBM as grade IV according to their classification of central nervous system tumours (*1*). Moreover, tumors in the supratentorial regions of the brain, such as cerebral hemispheres and midline structures, are the most common locations for GBM to arise in adults (*2*).

GBM diagnoses in adulthood have different survival rates depending on age of diagnosis. Those diagnosed between 20 and 44 years of age have 16.1% 5-year overall survival rates, which decreases with increasing age to less than 1% for patients diagnosed above 75 years of age, both representing dismal prognoses (*2*).

Almost 95% of GBMs arise *de novo* as primary lesions, whereas the other 5% (termed secondary GBMs) arise from pre-existing low-grade lesions, such as low-grade astrocytoma (LGA) (*3*). These two groups demonstrate distinct clinical courses, where primary GBMs typically manifest quickly after a short clinical history, while secondary GBM arise in a step-wise fashion from low-grade lesions over several years. Importantly, almost all adult low-grade astrocytoma will develop into secondary GBMs (*3*). Several studies, to be later described, have concluded primary and secondary GBM are in fact distinct disease entities developing from different genetic pathways.

As previously mentioned, adults with high-grade glioma have a universally dismal prognosis. Children diagnosed with high-grade glioma share a similarly poor outcome as adults, and thus it is important to understand specific genetic alterations characterizing adult high-grade glioma as well as pediatric high-grade glioma to review the genetic differences and similarities which should be considered when treating these patients.

1.1.2 The genetic landscape of primary adult GBM

Several studies have investigated the genetic landscape of primary GBM and uncovered distinct somatic point mutations and genomic copy number alterations that distinguish them from the secondary disease. For example, these tumors harbor genomic copy number gains of 1q, 12q (encompassing *MDM2*) and chromosome 7. Specific amplifications of receptor tyrosine kinases, such as *EGFR* and *PDGFRA* are also common. This group typically shows copy number loss of 16q as well as 10q. Importantly, a majority of these tumors harbor a focal deletion on chromosome 9, encompassing *CDKN2A* and *CDKN2B* tumor suppressor genes.

Several somatic point mutations also distinguish primary HGG. Mutations in the major tumor suppressor gene, *TP53*, are seen at a relatively low frequency (29% of cases) but the core

promoter of *hTERT*, which encodes the catalytic subunit of telomerase, is mutated at one of two hotspots (C228T; C250T) in over 80% of adult primary GBM. This suggests a major telomere maintenance mechanism utilized by these cancers. More specifically, these hotspot mutations generate *de novo* consensus binding motifs for ETS transcription factors that result in increased transcriptional activity from the *hTERT* promoter, perpetual elongation of telomeres and cellular immortality (*4*). It is important to note that these tumors rarely harbor point mutations in other genes such as *IDH1*, *IDH2* or BRAF V600E (*2*), whereas these mutations are enriched in secondary GBM.

1.1.3 The genetic landscape of adult secondary GBM

In contrast to adult primary high-grade glioma, secondary GBMs typically develop in younger patients from pre-existing low-grade glioma, and often contain an early *TP53* mutation, observed in more than 65% of cases. These secondary GBMs rarely show alterations or overexpression of *MDM2*, whereas it remains a genetic hallmark of primary glioblastoma. Other major genetic changes observed are *RB1* alterations, which are seen in roughly 39% of adult secondary GBM. This is in fact a comparable frequency to primary GBM (approximately 50%). However it's important to note that *CDKN2A* deletions are quite rare in secondary GBM (4%), in contrast to adult primary HGG where this is a common genetic event. *EGFR* amplification is also extremely rare in these tumors, highlighting another difference from the primary disease. Similar to primary HGG however, is amplification of the receptor tyrosine kinase, *PDGFRA*, which is recurrently amplified in secondary GBM (*5*). As these tumors evolve from pre-existing low-grade lesions, it is important to understand the early genetic hallmarks of their low-grade counterparts as well, and compare these alterations to what is seen in the pediatric setting.

1.2 Adult Low-Grade Glioma – genetic features

Many of the genetic hallmarks of secondary GBM are in fact early events in the transformation of these cancers, and can be traced back to their low-grade glioma counterparts. More specifically, these adult LGAs harbor early somatic mutations in IDH genes (*IDH1/2*), *TP53*, and *ATRX. ATRX* mutations strongly associate with alternative lengthening of telomeres or ALT, which is major telomere maintenance mechanism employed by cancer cells to overcome the "end replication problem" during DNA replication (*6*). As previously mentioned, these early alterations are rarely observed in primary HGG, and in fact underscore that specific genetic alterations like point mutations and copy number changes distinguish these two clinical subtypes.

Taken together, adult low-grade glioma have multiple early genetic aberrations and telomere lengthening mechanisms that contribute to their transformation to high-grade glioma, including somatic point mutations in IDH genes, *TP53*, *ATRX*, and ALT. These distinguish them from primary high grade glioma which typically have amplifications of *EGFR*, deletions of the major tumor suppressor genes *CDKN2A* and *PTEN*, *hTERT* promoter mutations and associated increased telomerase activity, among many others alterations.

Recent genomic studies have identified novel genetic alterations that distinguish pediatric from adult HGG, suggesting these are distinct diseases as well, and should be managed differently in the clinic. These studies, along with a clinical background of pediatric HGG, will be reviewed to highlight these differences.

1.3 Pediatric High-Grade Glioma

1.3.1 Clinical characteristics, outcome and mutational landscape

Pediatric patients with HGG have a dismal prognosis of less than 20% 2 years after initial diagnosis and are the leading cause of cancer-related death in children (*7, 8*). Although pediatric and adult HGG are virtually indistinguishable under the microscope, adult HGG are different as they usually arise in hemispheric locations, whereas childhood HGG arise in a broader spectrum of locations. Most notably, pediatric GBM remains essentially incurable despite decades of intensive therapeutic efforts (*9*).

The onset of the "genomic" era has allowed for the genomic landscape of these tumors to finally be investigated. Next generation sequencing efforts, such as whole-exome sequencing, has identified pediatric GBM to harbor a mean of 15 somatic non-synonymous mutations per tumor (range, 3 to 31) (*10*). Although genetic mutations in *TP53, CDKN2A* and *PIK3CA* are common in childhood and adult GBMs (*11-13*), there are also major differences in the genetic and molecular features of both groups (*10, 14-24*). Pediatric HGG do not harbor mutations in the IDH genes but instead have mutations in the histone H3 gene (*H3F3A*). This mutation results in a substitution of a lysine for methionine at residue 27, and arises frequently in DIPG (80%), and pediatric HGG of the thalamus and cerebellum (*25*). In contrast, pediatric HGG of the cerebral cortext harbor a missense mutation at residue 34 substituting a glycine for arginine or valine (*10, 26-28*). The K27M and G34R/V mutations occur at specific residues of the histone 3 tail and undergo post-translational modifications, such as methylation. These changes affect the epi-genome by influencing chromatin structure and gene expression (*10, 26*).

H3F3A G34 mutations frequently associate with *ATRX* mutations (*10, 28*). Mutations in *ATRX/DAXX*, which encodes two enzymatic subunits of a chromatin-remodeling complex required for H3.3 incorporation at pericentric heterochromatin and telomeres, are seen at a relatively high frequency of pediatric GBM, observed in 31% of cases (*10*).

Pediatric hemispheric high-grade glioma also harbor mutations (usually truncating) in *SETD2*, a H3K36 trimethylase, and appear mutually exclusive from H3.3 mutations (*10, 29*). Moreover, Strum *et al*. also identified *H3F3A* and *IDH1/2* mutations are mutually exclusive in GBM, as IDH mutations rarely occur in pediatric GBM and only in adults, as previously mentioned (*28, 30*). IDH mutations, such as IDH1 R132H, results in this enzyme producing increased levels of the onco-metabolite 2-hydroxyglutarate (2-HG). These increased enzyme levels inhibit histone demethylases, which results in increased methylation of H3K27 and H3K36, the two residues most frequently mutated in pediatric GBM (*10, 29*).

In general, *TP53* mutations occur in 42% of pediatric HGG and arise in many different anatomical locations, whereas deletions of the tumor suppressor gene *CDKN2A* occur only in non-brainstem HGG (*31*). Alterations in the p53 and/or RB pathways, two of the three major cancer pathways implicated in adult GBM, are found in 59% of pediatric HGG (*31*). Killela *et al*. have identified other recurrent somatic point mutations, specifically *hTERT* promoter mutations, which they observed in only 11% of pediatric primary GBMs (*32*). However this was based on a small cohort of only 19 patients (2 cases that were positive for an *hTERT* promoter mutation). Wu and colleagues found a much lower incidence of *hTERT* promoter mutations in primary pediatric GBM using a large cohort of 127 patients, with only 2% of DIPGs and 3% of non-brainstem HGG exhibiting one of the two mutations. Notably, only 4 of 58 non-brainstem

HGG had BRAF V600E mutations (7%), while no DIPG cases were positive for the mutation (*31*).

However, it is important to note that these studies do not distinguish between primary and secondary HGG in children. In contrast to the adult setting, malignant transformation of low-grade glioma to secondary HGG in children is rarely observed (*33*). However, pediatric high-grade glioma, regardless of clinical evolution, is a universally fatal disease, and thus it would be useful to identify early genetic markers that are unique to low-grade glioma experiencing transformation to mitigate that devastating outcome. This thesis serves to identify these markers, however a current understanding of the known clinical and genetic features of pediatric low-grade glioma is also necessary to give context to this study.

1.4 Pediatric low grade glioma

1.4.1 Clinical characteristics, survival, WHO grading, histological subtypes and management

Pediatric low-grade glioma (PLGG) is the most common central nervous system neoplasm in children under 19 years of age (*34-36*). These tumors are graded as I or II based on the WHO classification of central nervous system tumors, and are generally less aggressive and more responsive to therapy than high-grade glioma (*1*). PLGG is a chronic disease in which the timing, modality of therapy, and incidence of progression are all still very controversial. Unlike childhood malignant astrocytomas (WHO grade III or IV), PLGGs have a heterogeneous clinical course, ranging from long periods of growth arrest to nonstop progression (*37*). In contrast to the adult setting, where low-grade astrocytoma almost invariably undergoes malignant transformation to high-grade tumors (GBM), this event is quite rare in children (*33*).

As most children do not develop HGG after their PLGG diagnosis, the overall survival (OS) for these patients is excellent, observed at 86% (*34*).

PLGG comprise many histopathological subtypes, including pilocytic astrocytoma and ganglioglioma (both grade I) and diffuse astrocytoma and pleomorphic xanthoastrocytoma (both grade II). Small biopsies can result in difficulty in proper grading of PLGG, and are categorized by default as low-grade astrocytoma (LGA). Oligoastrocytomas are extremely rare in the pediatric setting, and for the purposes of this thesis, will not be discussed.

The anatomical location of PLGGs usually dictates extent of surgical resection. Most posterior fossa PLGGs can be almost completely resected, which usually results in excellent progression free survival (PFS) (*38*). Conversely, PLGGs located in midline structures such as the brainstem, optic pathways and spinal cord cannot be gross totally resected. The primary treatment modality for PLGG was radiation for many years, but concerns over the long-term sequelae have made physicians adopt more conservative approaches, such as low-dose chemotherapy and de-bulking strategies as the main approach to treating PLGG (*37*).

The WHO classification of CNS tumors however, does not always reliably predict biological behavior of low-grade glioma. Thus it is important to combine histological and clinical characteristics with the underlying genetics of these tumors in order to more effectively treat these patients. As such, a review of our current understanding of the genetic landscape of PLGG will be discussed.

1.4.2 The genomic landscape of PLGG: A single pathway disease

Before the genomic era, few genetic alterations were associated with PLGG development. Prior to 2008, germline loss of the *NF1* gene, an autosomal dominant predisposition syndrome termed

NF1, was one of the few alterations associated with this disease. More specifically, loss of function mutations in *NF1* is associated with pilocytic astrocytoma development. In particular, the protein product of *NF1*, neurofibromin, contributes to the growth arrest of astrocytic cells and neuronal differentiation by down-regulation of the mitogen-activated protein kinase (MAPK) signaling cascade through its GTPase-activating domain. Subsequent loss of this protein in patients with NF1 leads to increased RAS activity and cellular proliferation (*39*). Notably, NF1 patients usually develop PLGGs in the optic pathways.

In 2008, a landmark study by Pfister *et al*. used array-CGH to investigate copy number alterations in low-grade glioma in children. This group identified a novel duplication of chromosome 7, roughly 2 megabases (Mb) in length, (7q34), which encompasses the *BRAF* gene. The *BRAF* gene is a downstream target in the RAS-MAPK pathway (*40, 41*). To confirm a dosage effect resulting from this duplication, this group demonstrated that these tumors had increased mRNA levels of BRAF and a downstream target, CCND1, as compared with tumors without the duplication, suggesting aberrant signaling through the MAPK cascade (*40*). Soon after this finding, Jones *et al*. identified that the 7q34 duplication produces a novel oncogenic gene fusion with a constitutively active BRAF kinase domain. This was in fact the first report of a recurrent genetic alteration underlying the development of pilocytic astrocyoma, the most common histological subtype of PLGG. Specifically, the tandem duplication of 7q34 leads to a fusion of *KIAA1549* and *BRAF* genes. Using reverse-transcriptase PCR, three different breakpoints were observed by this group, which all retained the open reading frame encoding the BRAF kinase domain (*42*).

These fusion events result in constitutive activation of BRAF, and increased signaling through the MAPK pathway. However, constitutive activation of *BRAF* has also been seen to lead to

oncogene-induced senescence (OIS) in benign tumors, and has been supported by *in vitro* studies. More specifically, BRAF activation in human neural stem cells initially promotes clonogenic growth in soft agarose, suggesting partial transformation, but eventually stop proliferating and in fact show markers of OIS, such as expression of the p16 protein. As a consequence, OIS may be contributing to the less aggressive clinical course of PLGGs with the *BRAF* activation, but only in the absence of additional aberrations (*43, 44*).

The advent of the genomic era has led to the identification of many other genetic alterations in the MAPK pathway in PLGG. Specifically, whole-genome sequencing of 39 PLGGs has characterized their genomic landscape, observing a median of only 1 somatic non-silent alteration per PLGG. The most common genetic alterations identified were copy number alterations, gene rearrangements and activating mutations in *BRAF, RAF1, FGFR1, MYB* and *MYBL1 (45)*, which are all involved in MAPK signaling.

In fact, almost all genetic alterations identified in PLGG affect members of the MAPK pathway, and suggest this tumor is a single pathway disease. With respect to specific clinical features associated with identified genetic alterations in the MAPK pathway, those PLGG with the 7q34 duplication usually have a more favorable progression-free survival than those PLGG that do not harbor this alteration (*37*). Notwithstanding this single finding, few clinical characteristics have been associated with the other identified alterations. Most importantly, no genetic alterations have been associated with malignant transformation of PLGG, which is a major cause of death for these patients. The fact that fusion events involving the *BRAF* gene are very common, and have been associated with favorable progression free survival, suggests other alterations in the *BRAF* gene may also be useful for predicting the clinical behavior of PLGG.

1.4.3 Over-activation of the MAPK pathway resulting from the BRAF V600E point mutation

The most potent activator of the mitogen-activated protein kinase (MAPK) pathway is the v-raf murine sarcoma viral oncogene homolog B1 (BRAF). Strikingly, the RAS/BRAF/MEK/ERK pathway is mutated in approximately 30% of cancers, with 7% of cancers harboring an activating mutation in the BRAF gene (*46, 47*). More specifically, oncogenic activating mutations, such as BRAF V600E, which involves a thymidine to adenosine transversion (c.1799C>T), account for over 90% of mutations in BRAF (*46*). This mutation was first described in melanoma, colon, and papillary thyroid carcinoma (*48, 49*). *BRAF* mutations most frequently affect the 600^{th} codon (in exon 15) and are characterized by the amino acid substitution of valine by glutamate. The *BRAF* V600E mutation is thought to mimic the phosphorylation of the activating amino acid T599 and S602, thereby resulting in continuous activity of the mutant protein. As mentioned previously, the BRAF protein is responsible for transmitting extra-cellular signals to promote cellular proliferation, differentiation and survival (*47*).

BRAF is one of 3 members of the RAF family, which also includes ARAF and CRAF, all of which are serine/threonine kinases. Notably, BRAF has the highest basal level of all other members of the RAF family. As previously mentioned, BRAF regulates the MAPK pathway by transducing extra-cellular signals to the nucleus. These extracellular signals include cytokines, hormones and growth factors that interact with their extra-cellular receptors to recruit and activate G-proteins of the RAS family to the cytoplasmic side of the cell membrane. Activated RAS uses adaptor proteins to activate and recruit RAF proteins to the cell membrane. BRAF then signals to MEK and ERK via specific serine/threonine phosphorylation, to activate

downstream transcription factors involved in a range of biochemical processes including cellular growth, apoptosis, differentiation and proliferation, as previously outlined (*50*).

Although BRAF V600E is a common oncogenic activating mutation in PLGG, it is not observed at the same frequencies across all histological subtypes. In fact, the mutation is rarely observed in pilocytic astrocytomas, which are instead characterized by the 7q34 duplication, whereas pleomorphic xanthoastrocytoma and ganglioglioma are enriched for the mutation. As such, further discussion of the histological subtypes enriched for the mutation is warranted, as are the cell types that typically demonstrate the mutant protein.

1.4.4 Histological distribution of PLGG with recurrent oncogenic BRAF mutations

Histological subtypes of PLGG including ganglioglioma and pleomorphic xanthoastrocytoma harbor the oncogenic *BRAF* mutation, while it is rare in other subtypes. More specifically, approximately 66% and 18% of pleomorphic xanthoastrocytoma and ganglioglioma harbor this mutation respectively (*51*).

Ganglioglioma is in fact a glio-neuronal tumor composed of two different cell types. These are neoplastic glial and neuronal components. However, there is controversy regarding which cell type demonstrates neoplasia. Immunohistochemistry on 71 gangliogliomas using the monoclonal antibody VE1 localized the BRAF mutant protein predominantly in the neuronal compartment, suggesting the *BRAF* mutation occurs in cells that have the ability to differentiate into ganglionic cells. However, this group also identified this mutant protein in a small proportion of glial cells (*52*).

Further investigation using the same methods, being immunohistochemistry, identified ganglioglioma with the BRAF V600E mutation to be associated with shorter recurrence-free survival, and is thus a negative prognostic indicator in the pediatric setting (*53*). Increased expression of phospho-ERK, a downstream target of *BRAF*, was identified using immunohistochemistry in PXAs, suggesting again that MAPK pathway activation is important in this histological subtype as well. Indeed, the *BRAF* mutation is the hallmark genetic lesion of both ganglioglioma and PXA (*54*).

1.4.5 Clinical treatment using the BRAF mutant small molecule inhibitor

Patients with PXA and ganglioglioma that harbor the BRAF V600E mutation may be suitable for targeted therapy using the BRAF inhibitor, such as vemurafenib (PLX-4032). In fact, inhibition of the mutant protein with vemurafenib has been shown to improve the survival of melanoma patients (*55*). However there has been little clinical experience in children using the drug, aside from a case report of a ganglioglioma successfully treated with the drug. *In vitro* and *in vivo* investigations of pediatric astrocytoma cell lines harboring the mutation treated with the drug shows significant growth arrest, further supporting the use of this drug in the clinical setting (*56*). However, one could speculate that the drug would be less effective for those patients diagnosed with PXA, as this subtype, as well as high-grade childhood astrocytomas, has been showed to harbor additional genetic alterations, such as in the RB1 tumor suppressor pathway in addition to BRAF mutations.

1.4.6 RB pathway abnormalities with MAPK pathway over-activation

Weber and colleagues investigated genomic copy number alterations of PXA to determine if alterations in addition to oncogenic *BRAF* were contributing to this disease. Using comparative

genomic hybridization, they identified the most recurrent chromosomal imbalance to be a focal deletion of chromosome 9 (9p21.3), encompassing the tumor suppressor gene *CDKN2A,* present in 50% of their cases. They further confirmed their findings using interphase fluorescent in situ hybridization (*57*).

Zhang *et al.* also confirmed the previous groups findings that *CDKN2A* deletions are the most recurrent focal copy number change in PXAs, which was identified in 70% of their cases (7/10). Interestingly, they identified 6 of 7 PXA cases to harbor concomitant *CDKN2A* deletions and *BRAF* V600E mutations (*45*).

Similar to PXA, malignant astrocytoma of childhood has been shown to harbor these two alterations as well. In 2010, Schiffman *et al.* identified 5/31 (16%) childhood malignant astrocytomas to harbor the BRAF V600E mutation, suggesting these tumors constitute a distinct genetic subset. However, no clinical outcomes based on *BRAF* status were investigated (*18*). Interrogation of copy number alterations by Schiffman and colleagues further uncovered that 3/5 malignant astrocytoma harbored deletions of the tumor suppressor gene *CDKN2A* concurrently with *BRAF* V600E (*18*).

In the following year, Schindler *et al*. sequenced 1,320 central nervous system tumors from adults and children, and observed the *BRAF* mutation occurred in only 6% of their adult secondary GBM cases. As secondary GBMs from children are extremely rare, none were tested for the mutation (*51*).

These findings underscore not only the importance of MAPK pathway activation in PXAs and malignant astrocytomas of childhood, but also the RB pathway. The gene product of *CDKN2A*, p16, is a critical regulator of the RB tumor suppressor pathway. In fact p16 functions as a

regulator of G1/S phase transition by inhibiting the activity of cyclin-dependent kinases Cdk4 and Cdk6 (*57, 58*). With the knowledge that PXAs, which have a tendency to transform to high-grade tumors, as well as malignant astrocytomas showing aberrant signaling of MAPK and RB1 cancer pathways, it begs the question whether other glioma with these alterations will have more aggressive clinical behaviors. However, few clinical characteristics have been associated with BRAF V600E and *CDKN2A* deletions and the other major genetic alterations of PLGG, particularly no alterations have been associated with malignant transformation.

1.5 Malignant transformation of pediatric low-grade glioma

1.5.1 Early evidence of the role of radiation and cancer predisposition syndromes in transformation of glioma

Few studies have investigated the clinical or genetic features involved in transformation of low-grade glioma in children, however low-grade astrocytoma have been reported to develop anaplastic changes after patients receive radiation treatment. Most of these tumors were located in the optic pathway, and not in hemispheric regions. More specifically, in 1994, Dirks *et al.* reported their experience with 6 children who received radiotherapy treatment for low-grade astrocytoma, which then progressed to anaplastic astrocytoma. The mean initial age of diagnosis for all patients was 5.3 years old. Notably, 5 of the children were initially treated with radiation and underwent surgery. The sixth child received only radiation. The mean latency period to transformation was 6.4 years, with a range of 2 to 10 years. All high-grade recurrences were located in the primary site or within the radiation field. After histopathological review, 4/6 children were diagnosed as anaplastic astrocytoma, while the remaining patients were diagnosed with GBM. This group concluded that radiation played an integral role in the malignant

transformation of low-grade astrocytoma. Interestingly, one of these patients was previously diagnosed with NF1 syndrome. Notably, this group observed no malignant changes of low-grade astrocytoma in the absence of radiation (*59*).

Another early report of PLGGs with aggressive progression was a study investigating pilocytic astrocytomas by Krieger et al. in 1997. They observed 11% of pilocytic astrocytomas (4/36) were diagnosed as anaplastic astrocytoma at recurrence. Three of 4 of these children received radiation and/or chemotherapy, with only 1 of them showing disease progression without treatment. After histopathological review, increased perivascular cellularity was identified in a majority of low-grade tumors, whereas only 2 of 32 PLGG that did not transform also showed this feature. This group concluded that early perivascular cellularity could be indicative of a more aggressive clinical course for PLGG, however no other risk factors were identified (*60*).

Most NF1 patients who develop pilocytic astrocytoma rarely experience malignant transformation as their tumor remains at WHO grade I status. However, case reports of NF1 patients with low-grade glioma experiencing malignant transformation have been reported (*61*). An important investigation in 2006 published in the *Journal of Clinical Oncology* studied the long-term risk of occurrence of second tumors in NF1-related optic pathway gliomas following radiotherapy. They identified that 7/18 patients who were irradiated developed secondary tumors, compared to 8/40 non-irradiated tumors, giving a risk of 3.9% versus 1.2% of developing a second tumor per year, respectively. Moreover, no patients from the non-irradiated group died from their secondary tumors, whereas 5 of 18 patients from the irradiated group did die from their secondary tumors. This group concluded that there is a significant risk of second central nervous system tumors in NF1 patients who receive radiation therapy for their optic pathway gliomas, suggesting radiation should be used sparingly (*62*). However, 20% of patients

that were not treated with radiotherapy developed second tumors after their initial low-grade glioma diagnosis, suggesting malignant changes are not solely induced by radiation alone. This underscores the need to uncover the biological mechanism non-irradiated low-grade glioma use to experience malignant changes (*62*).

1.5.2 Molecular and clinical determinants of PLGG transformation: What's known?

Before the genomic era, a seminal paper published in *the Journal of Clinical Oncology* by Broniscer and colleagues described, for the first time, molecular and clinical features of pediatric low-grade glioma transformation. An in-depth review into this study is important to understand what is currently known about this rare but important phenomenon in the pediatric setting. Importantly, this group only investigated genetic and molecular alterations known in gliomagenesis for their analyses (*33*).

This group investigated a small cohort of 165 patients at their institution that met study criteria for transformation of PLGG. They identified 11 patients of 165 who met study criteria, an incidence of approximately 7%. The median age at initial diagnosis was 13.3 years, with 6 of 11 children receiving radiation therapy at PLGG diagnosis. Interestingly, no risk factors assessed, including radiation therapy, tumor location, extent of resection or use of chemotherapy was found to be associated with increased incidence of transformation (*33*).

With respect to somatic genetic variants, this group investigated only the major tumor suppressor gene *TP53*. Briefly, in non-cancerous cells, the p53 pathway is responsible to respond to cellular stress, usually triggered during aberrant DNA replication or cell division. Post-translational modifications of the p53 protein are triggered by a molecular stress signal,

resulting in the activation of the protein as a transcription factor that begins cell cycle arrest, cellular senescence or apoptotic programs. Single nucleotide variants or copy number loss of the *TP53* gene, frequent in cancer cells, can result in stabilization of the protein and an inability to send downstream signals to activate the aforementioned programs, resulting in the inability to induce apoptosis in these cells (*63*).

Broniscer *et al*. identified 1 of 6 of their PLGGs and 2 of 6 HGG to harbor deleterious mutations in *TP53*. The one patient with paired samples acquired a mutation only after malignant transformation, suggesting *TP53* mutations were late events in this particular cohort, although this was only one such example. P53 overexpression was more common following transformation, however their small cohort precluded them from drawing any statistically significant associations. In contrast to most PLGGs, 71% of their low-grade tumors that went onto transform harbored alterations in the RB tumor suppressor pathway, either being deletions of *CDKN2A* and/or *RB1* deletions. Moreover, nine of 10 HGGs demonstrated alterations in this same pathway. Notably, amplification of *PDGFRA* was identified in only 1 patient following transformation (*33*).

This group concluded that genetic alterations in their cohort following transformation were similar to those identified in adult primary and secondary glioblastoma, specifically alterations in the retinoblastoma tumor suppressor pathway. However, their small cohort prohibited them from identifying recurrent genetic or molecular variants or risk factors predisposing low-grade glioma to transformation (*33*). Quite strikingly, no further investigations into the genetic, molecular or clinical characteristics of this rare patient cohort have been conducted since this important study in 2007. Currently, there is an urgent need to define the risk of transformation of PLGG on a population-based cohort, to use a discovery-based genomic platform on

secondary high-grade glioma in children, and determine whether specific genetic events occur early on in the transformation of these tumors. As such, therapy could be tailored to specific genetic or molecular subgroups of PLGG that are at higher risk for transformation.

1.6 Project Rational and Hypothesis

Pediatric low-grade gliomas are the most prevalent central nervous system neoplasm. Unlike malignant primary high grade gliomas (e.g. GBM) of childhood, which progress relentlessly and are invariably lethal, PLGGs have a heterogeneous clinical course, ranging from prolonged periods of growth arrest to continuous progression and, in some cases, malignant transformation to secondary high grade glioma (sHGG).

Currently, PLGGs are treated in a similar fashion, as few biological makers are available to allow stratification of therapy. Thus, there is an urgent need for clinical and biological risk stratification for these children so clinicians can know who to treat, how aggressively to treat them, and what targeted agents to use, especially for the group of patients whose PLGGs will experience malignant transformation to secondary high-grade glioma. There is also a need to define the risk of transformation of PLGG using a population-based cohort with long clinical follow-up.

The genetic and molecular determinants of low-grade glioma transformation in children remain largely uncharacterized. Furthermore, few clinical outcomes have been associated with specific genetic or molecular markers to aid physicians in risk stratification to guide the clinical management of PLGGs. As such, we **hypothesize** that secondary high-grade glioma are genetically distinct from primary high grade glioma in children, these distinct genetic alterations are in fact early events in the transformation of pediatric low-grade glioma, and genetic subgroups of PLGG which experience transformation have distinct clinical outcomes.

Therefore, the objectives of this thesis were:

1. To determine the prevalence of transformation in a population-based cohort of PLGG with long clinical follow-up.

2. To uncover the genomic and genetic alterations which define pediatric secondary high-grade glioma (sHGG).

3. To determine which of these genetic alterations are early events in malignant transformation of pediatric low-grade glioma (PLGG).

4. To identify clinically distinct genetic or molecular subgroups for patient risk stratification that may mitigate the devastating transformation event.

In order to uncover genetic alterations in pediatric sHGG, we first identified all patients treated for PLGG at a single institution in a population-based manner at the Hospital for Sick Children. Specifically, SickKids is the only referral center serving a population of more than 10 million people, thus serving as a population-based cohort and eliminating referral bias. Detailed clinical data for patients treated for PLGG who met study criteria for transformation was ascertained from chart reviews. Using a discovery-based approach, we used whole-exome sequencing and array-CGH on the largest cohort of sHGG to date and validated for recurrent alterations in an overlapping, expanded cohort of sHGG.

In order to determine if recurrent alterations in sHGG were indeed early events in transformation, we collected tissue from all PLGG that underwent transformation. We subsequently interrogated sHGG for recurrent mutations and copy number alterations, and then

in patient-matched and non-matched PLGGs, to determine if these alterations were indeed early events.

In order to identify genetic subgroups with distinct clinical outcomes, we collected extensive clinical data relating to age, latency to transformation and survival and correlated with genetic and molecular data to develop a risk stratification algorithm for patients with PLGG.

2 CHAPTER 2: MATERIALS AND METHODS

2.1 Methods Workflow - Overview

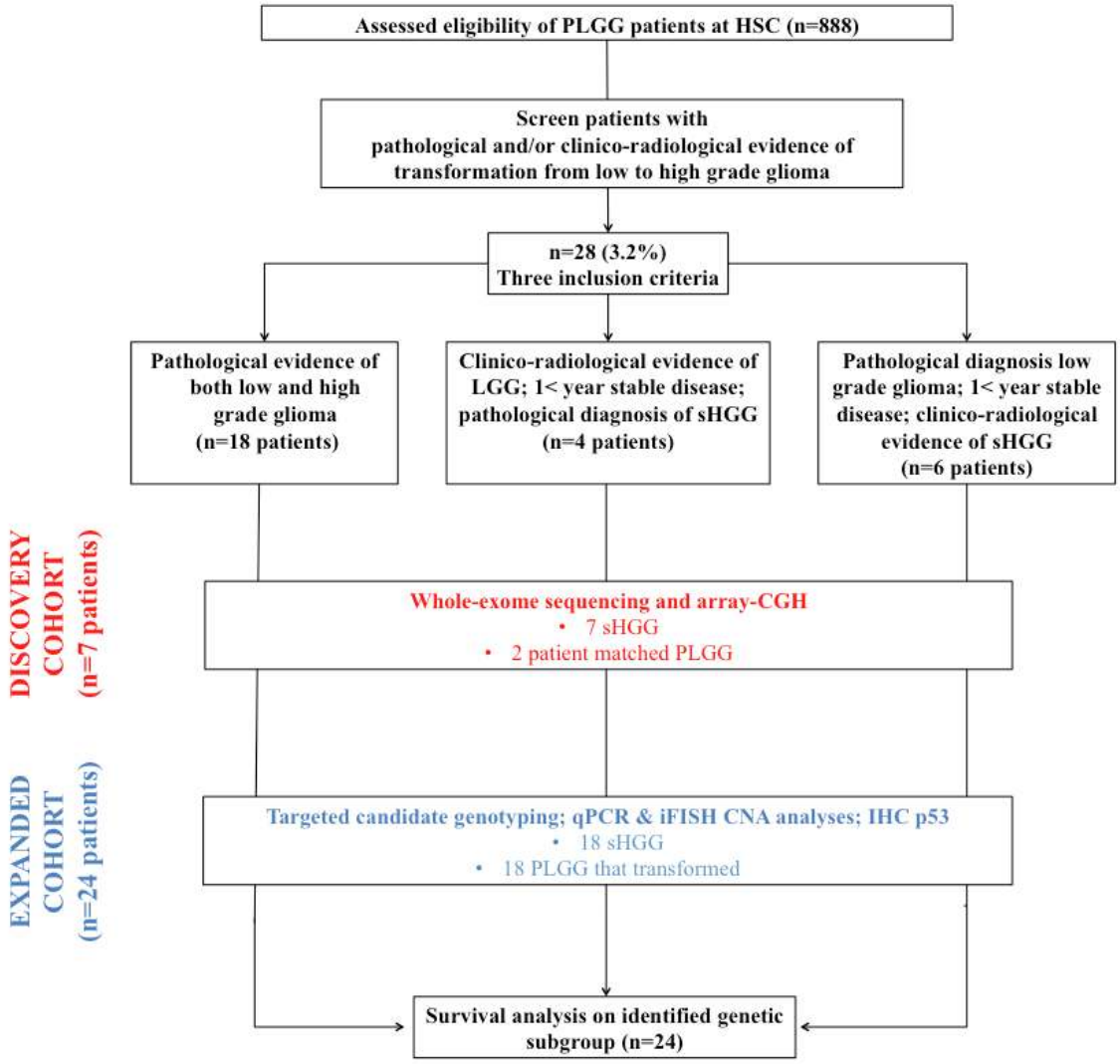

Figure 2.1: Methods Workflow Overview. The above workflow is an overview of the methods used for identifying transformation at the Hospital for Sick Children, with corresponding sample sizes. PLGG-MT refers to those PLGG experiencing malignant transformation. The expanded cohort includes those patients from the initial discovery cohort.

2.2 Patient Characteristics and Tumor Samples

Following institutional review board approval, all patients treated at the Hospital for Sick Children (SickKids), Toronto, Ontario, Canada, for PLGG between January 1, 1986 and December 31, 2013 were reviewed for malignant transformation. As SickKids is the only referral center in a population serving over 10 million people in Southern Ontario, no selection bias is expected, and this qualifies as a population-based study. Furthermore, the Ontario health system tracks clinical outcome data on all residents enabling us to collect long term follow-up data including transformation events and survival for >97% of patients including adults until December 2013. There were 28 patients that were identified for PLGG transformation. There were 18 patients with matched consecutive low and high grade histological diagnoses as per the WHO 2007 criteria (*1*); 6 patients had low grade histological diagnosis, followed by high grade diagnosis as determined by radiologic evidence; 4 patients had radiologic evidence of low grade disease, at least 1 year stable disease, followed by histological high grade diagnosis (**Figure 2.1**). Demographic, treatment and outcome data were ascertained from our PLGG database as previously described (*37, 64*).

Tumor tissue for genetic and molecular analyses was available from 18 low grade glioma which underwent transformation and 18 secondary high grade tumors, from a total of 24 patients. 4 patients had no tissue available. There were a total of 6 patient matched control tissues used from 7 patients with sHGG, including 5 peripheral blood samples and 1 fibroblast cell line. Tumor tissue from 31 primary high-grade glioma (non-brainstem) samples and 167 PLGG that did not transform (randomly chosen) were also collected for correlative studies. However, all PXA cases at our center were included in this cohort of 167 PLGG. Genomic DNA was extracted from formalin-fixed paraffin embedded tumor tissue utilizing the RecoverAll Total

Nucleic Acid Isolation Kit (AM 1975) according to instructions from the manufacturer (Life Technologies). Genomic DNA was also extracted from snap frozen tumor tissue and peripheral blood utilizing the Qiagen DNeasy Blood and Tissue kit according to instructions from the manufacturer (Qiagen) (*65*).

2.3 Whole-exome sequencing – mutational analyses

Whole-exome sequencing (WES) was performed on a discovery cohort of 7 sHGG, 2 patient matched PLGG and 5 patient matched germline samples at The Center for Applied Genomics (TCAG) at the Hospital for Sick Children (7 patients total). No germline tissue was available for 1 patient (#19) so the patient's low grade tumor was used as the control to call somatic mutations in the high grade counterpart. Another patient (#7) developed myeloid dysplastic syndrome so a matching fibroblast cell line from the same patient was used as a control to call somatic mutations in the sHGG (total n=7 sHGG with matching control tissue to call somatic variants) (**Figure 2.1**).

3-6µg of genomic DNA was submitted for target capture with the Illumina TruSeq exome enrichment kit (Illumina) and 100 bp paired-end sequencing reads on the Illumina 2000 HiSeq platform (Illumnia) with bioinformatics processing and variant annotations as previously described at TCAG (The Hospital for Sick Children). Sequence were aligned to the reference human genome hg19 with BWA 0.5.9; MarkDuplicates (picard-tools-1.79) was used to remove any duplicate paired-end reads and the subsequent duplicate-free alignments were refined using GenomeAnalysisTK (GATK) 1.1-28; base quality recalibration was also performed using (GATK) 1.1-28. Somatic variant calling was performed using MuTect v1.1.4 with cosmic v63 (Broad Institute) (*66*). Mutation totals for sHGG were calculated by including only those SNVs

identified in the tumor and not in the matching germline tissue and mutations predicted to be potentially deleterious by changing the coding of a protein (i.e., nonsynonymous coding, stop codon lost, and stop codon gain mutations). Mutation totals of pHGG were taken from a previously published study (*31*).

2.4 Sanger sequencing analyses

We investigated candidate somatic point mutations and glioma hotspots in a validation cohort of patients for which genomic DNA was available. 50 ng of genomic DNA from patients was used to amplify exon 15 of *BRAF*, exon 4 of *IDH1* and exon 2 of *H3F3A* with the use of a polymerase-chain reaction (PCR) assay as previously described. 5µl of PCR product was treated with 2µl Exo-SAP-IT (Affymetrix) and sequenced using the Sanger method as previously described (*21, 26, 40*). Sequencing chromatograms were manually curated for hotspot mutation detection.

2.5 Genotyping for BRAF and hTERT promoter mutations

The *BRAF* mutation status was determined with commercially available TaqMan Mutation Detection Assay (Applied Biosystems). Competitive allele-specific TaqMan PCR (castPCR) using the BRAF_476_mu probe for the detection of the *BRAF* c.1799T>A mutation were run in triplicates on an Applied Biosystems 7900HT Fast Real-Time PCR System. The mutant allele frequency was determined by comparing the cycle threshold (C_t) values of the wild-type and mutant allele assays (ΔC_t) in reference to the control samples using Mutation Detector software 2.0. The percentage of mutant *BRAF* alleles was calculated as $\%=1/(2^{\Delta Ct}) \times 100$ (*67*). All *BRAF* mutant positive samples by Sanger were validated by castPCR.

Two primers (forward primer, 5′- CAG CGC TGC CTG AAA CTC -3′; reverse primer, 5′- GTC CTG CCC CTT CAC CTT C -3′) were designed to amplify a 163-bp product encompassing C228T and C250T hotspot mutations in the *TERT* promoter – corresponding to the positions 124bp and 146bp, respectively, upstream of ATG start site. Two fluorogenic LNA probes were designed with different fluorescent dyes to allow single-tube genotyping. One probe was targeted to WT sequence (*TERT* WT, 5′-5HEX-CCC CTC CCG G -3IABkFQ-3′), and one was targeted to either of the two mutations (*TERT* mut, 5′-56FAM-CCC CTT CCG G -3IABkFQ). Primer and probe design was performed by using Primer Express software, version 3.0 (Applied Biosystems, Burlington, ON, Canada), and sequence homogeneity was confirmed by comparison to all available sequences on the GenBank database by using BLAST (http://www.ncbi.nlm.nih.gov/BLAST/). Primers have been checked for hairpins, homo- and hetero-dimers. Primers and probes were obtained from Integrated DNA Technologies (Coralville, Iowa, USA).

Real-time PCR was performed in 25-µl reaction mixtures containing 12.5 µl of TaqMan Universal Master Mix II with UNG (Applied Biosystems), 900 nM concentrations of each primer, 250 nM *TERT* WT probe, 250 nM *TERT* MUT probe, and 1 µl (25 ng) of sample DNA. Thermocycling was performed on the StepOnePlus (Applied Biosystems) and consisted of 2 min at 50°C, 10 min at 95°C, and 40 cycles of 95°C for 15 s and 60°C for 1 min.

Analysis was performed by using StepOne Software, version 2.1. Samples were considered mutant if they had CT values of ≤39 cycles. Each sample was verified visually by examining the PCR curves generated to eliminate false positives due to aberrant light emission. End-point allelic discrimination genotyping was performed by visually inspecting a plot of the

fluorescence from the WT probe versus the MUT probe generated from the post-PCR fluorescence read (*68*).

2.6 Comparative genomic hybridization data analysis

Genomic copy number alterations (CNA) of tumor samples from the same discovery cohort used for WES (7sHGG and 2 patient matched PLGG; **Figure 2.1**) were profiled using CytoSure ISCA array (ISCA v2 4X180K) by Agilent. Feature extraction files were analyzed for CNAs using Partek Genomics Suite (PGS) version 6.6 (Partek Incorporated, St Louis, MO). Briefly, LogRatio values were imported into PGS and normalized using quantile normalization. Copy number data was generated from Log_2 ratio values. The genomic segmentation and HMM tools available from PGS were used to determine regions of gains and losses with copy number >2.5 considered a gain and <1.5 considered as a loss. A high level gain was considered equal to or greater than 5. Homozygous deletions were considered below 0.5. Only genes with CNAs reported by both algorithms were included in the results. CNA genome rates per sample were reported using genomic segmentation algorithm. We investigated copy number changes for all genes covered on the array as well as specific gliomagenesis genes of interest, including: *CDKN2A, FGFR1, BRAF, NF1, TP53, RB1, PTEN, PDGFRA, MYB, MYBL1, EGFR, MDM2* and *ATRX*. *CDKN2A* was the only CNA validated using qPCR.

2.7 Copy number assays for CDKN2A deletions – Real-time quantitative PCR

The copy number for *CDKN2A* was determined using 2 commercially available and pre-designed TaqMan Copy Number Assays according to the manufacturer's instructions (Applied

Biosystems). The primer IDs used for *CDKN2A* were Hs03714372_cn and Hs00965010_cn. The human RNase P H1 RNA gene was used as an internal reference copy number. Real-time quantitative PCR (in quadruplicates) was performed in a total volume of 20µl in each well, containing 10µl of TaqMan genotyping master mix, 20ng of genomic DNA and each primer. The PCR conditions were 95°C for 10 min and 40 cycles of 95°C for 15 s and 60°C for 1 min; the resulting products were detected using the ABI PRISM 7900HT Sequence Detection System (Applied Biosystems). Data was analyzed using SDS 2.2 software and CopyCaller software (Applied Biosystems). The *CDKN2A* deletion status shown in Figure 1 was obtained from qPCR results. Only the Hs03714372 assay was used for correlative studies (Figure 2). Only 1 deletion from CGH array analysis did not validate using qPCR (D909 from patient 18) (*69*).

2.8 Immunohistochemistry of p53 and BRAF V600E

These studies were performed on 5µm-thick, formalin-fixed, paraffin-embedded tissue sections either as single samples or combined as tissue microarrays containing 1-mm cores derived from the respective tumor blocks. Immunohistochemical studies for the p53 protein were performed using standard techniques as previously reported (*70*). Immunohistochemical studies for the *BRAF* V600E mutation were performed using the *BRAF* V600E mutant-specific antibody, VE1 as previously described (*53*). Positive and negative staining was evaluated using light microscopy by a neuropathologist from SickKids (C.E.H.).

2.9 Alternative lengthening of telomeres (ALT) by c-circles

ALT was detected by screening for c-circles. C-circles are extrachromosomal telomeric repeats (ECTRs) which are ALT specific. They have been found to be robustly associated with ALT and are present in tumors which maintain their telomeres using a recombination phenotype, even

following loss of other ALT phenotypic markers(*71*). C-circles were detected using a telomere-specific qPCR assay (*72*).

DNA was diluted to 3.2 ng/µL. 16 ng (5 µL) of DNA was treated with 5 µL of Φ29 master mix containing: 4 mM DTT, 10x Φ29 buffer, 10 µg/µL BSA, 0.1% Tween, 1 mM (each) of dATP, dGTP, dTTP and dCTP, 5 U of Φ29 polymerase.

Following the Φ29 amplification, the samples were diluted to 0.4 ng/µL by adding 30 µL of sterile water to the reaction mixture. Un-treated dilutions of 0.4 ng/µL were also prepared.

The qPCR assay was run with triplicates of Φ29 treated and untreated DNA, requiring a total of 6 PCRs per sample. Each qPCR required 15 µL of master mix and 5 µL (2 ng) of DNA. qPCR master mix contained: 1x QuantiTECT SYBR Green Master Mix (LifeTechnologies - 4309155), 10 mM DTT, 0.5 µL DMSO, and 300 nM of forward primer and 400 nM of reverse primers.

All qPCRs were done in 96 well plates using the Lightcycler 480 (Roche). PCR conditions were: 95 °C for 15 minutes, 35 cycles of 95 °C for 15 seconds (denaturation), and 54 °C for 2 minutes (annealing and elongation). Lightcycler 480 software was used to obtain data.

For determining presence of c-circles, a ΔmeanCp value was calculated for each sample. The ΔmeanCp was the difference between the mean values of the non-Φ29 and Φ29 treated samples. A positive ΔmeanCp value greater than 0.2 was detected in c-circle positive samples, whereas a negative ΔmeanCp value of less than -0.2 was detected in c-circle negative samples. Samples with ΔmeanCp -0.2 – 0.2 were considered as atypical, and results were confirmed using the dot blot.

2.10 Statistical analysis

Statistical analysis of Fisher's exact test (correlative studies) was performed using GraphPad Prism software v6.0 ($P<.05$ was considered significant). The unpaired two tailed Student t tests was conducted using Microsoft Excel v14.3.7. Survival analyses were done using the Kaplan-Meier method. Multiple hypothesis testing was accounted for in determining significance. A log-rank test was used to compare groups and curves were generated using Stata v12.

3 CHAPTER 3: RESULTS

3.1 Clinical characteristics of low grade glioma transformation in children

Of 888 patients treated at our institution for PLGG, 28 patients (3.2%) fulfilled study criteria for MT. There were 14 males and 14 females enrolled in the study. Seventy-five percent of tumors were hemispheric and thalamic in origin. The remaining tumors were located in the brainstem (22%) and the optic pathway (3%). The median latency to MT was 2.19 years (range, 0.32 to 20.3 years) (**Table 3.1; Appendix A**).

The major histological subtypes of PLGGs were pilocytic astrocytoma and grade I low grade astrocytoma's, comprising 35% of PLGG each, while the remaining tumors were pleomorphic xanthoastrocytomas (22%) or gangliogliomas (8%). The 2 major histological subtypes at MT diagnosis were anaplastic astrocytoma (39%) and GBM (30%). The remaining sHGG were anaplastic pleomorphic xanthoastrcytoma (22%) and anaplastic ganglioglioma (8%). 3 tumors (all sHGG) were disseminated at diagnosis, 2 of which were located in hemispheric regions. No PLGG was disseminated at diagnosis (**Table 3.1; Appendix A**).

Of PLGG that underwent surgical resection, a majority had sub-total resections (n=15). One had a gross-total resection, 1 had a partial resection, and 6 had biopsies only. Sub-total resections were also the most common form of surgery at MT diagnosis (n=5), followed by biopsy (n=4), partial resection (n=3), and only 1 tumor with a gross-total resection. 5 sHGG had surgery, but the extent was unknown. 10 sHGG did not have any form of surgery (**Table 3.1; Appendix A**).

The median age at PLGG diagnosis for all patients was 6.9 years (range 0.38 to 15.6 years). The median age at MT was 11.7 years (range, 0.57 to 33.7 years). Only 7/28 (25%) patients were treated with radiotherapy at PLGG diagnosis, which had a median survival of 1.27 years (range, 0.67 to 4.03 years) after diagnosis, slightly lower than that of all patients (3.37 years; range, 0.52 to 26.1 years) (**Table 3.1; Appendix A**).

Radiotherapy was given to 7 PLGG and 14 sHGG following diagnosis. Three patients (11%) had cancer predisposition syndromes. These included one patient with NF1, one with Li-Fraumeni Syndrome (LFS) and one with biallelic mismatch repair deficiency syndrome (bMMRD). The median survival following MT for all patients was 0.80 years (range, 0.1 to 21.7 years). Twenty-five of 28 patients (89%) died from tumor progression (**Table 3.1; Appendix A**).

Characteristic	Patients	
Gender (male/female)	14/14	
Tumor location (No.)		
Hemispheric	11	
Thalamic	10	
Brainstem	6	
Optic pathway	1	
Median latency to MT, years, (range)	2.7 (0.32-20.3)	
Outcome (No.)		
Alive/Deceased	3/25	
	PLGG	**sHGG**
Disseminated at diagnosis	0	3
Histologic diagnosis (No.)		
Low grade astrocytoma	8	
Pilocytic astrocytoma	8	
Pleomorphic xanthoastrocytoma	5	
Ganglioglioma	2	
Anaplastic astrocytoma		9
Glioblastoma mulitforme		7
Anaplastic pleomorphic xanthoastrocytoma		5
Anaplastic ganglioglioma		2
Extent of surgical resection (No.)		
Gross-total resection	1	1
Sub-total resection	15	5
Partial resection	1	3
Biopsy	6	4
Surgery done (extent unknown)	0	5
Surgery not done	5	10
Treated with RT after diagnosis (No.)	7	14
Chemotherapy received (No.)	9	17
Median age diagnosis, years, (range)	6.9 (0.38-15.6)	11.7 (0.57-33.7)
Median OS post diagnosis, years, (range)	3.37 (0.52-26.1)	0.8 (0.1-21.7)

Table 3.1: Summary of patient and tumor characteristics, treatment and outcomes of patients with low grade glioma transformation in children. Patient characteristics comprise the first half, while tumor characteristics comprise the bottom (PLGG and sHGG).

3.2 The landscape of somatic point mutations in secondary high grade glioma

3.2.1 Somatic mutation load in secondary high grade glioma

Mean sequencing coverage of sHGG and matched control tissue (n=7 pairs) was 94x and 114x respectively. Three patients with cancer predisposition syndromes were included in the cohort, however no tissue was available for 1 patient with NF1. A LFS patient (#7) harbored 21 somatic mutations in their sHGG. Another patient (#16) harbored 11,953 somatic mutations, representing a hypermutator phenotype (HPM), in their sHGG. Mutation analysis using exome data of the matching germline tissue of this patient revealed biallelic mutations of the mismatch repair gene *PMS2* (p. R421X; D544N) and in fact was diagnosed previously with the cancer predisposition syndrome bMMRD. Perhaps not surprisingly, this patient's PLGG also harbored a relatively high mutation load (13 somatic mutations).

Exome analysis identified a median somatic non-silent mutation rate of 0.45/Mb in 7 sHGG (median, 25). This median number of mutations is over twice as high as in primary HGG, as previously identified in published sequencing data (median, 11; p=0.0042) (**Figure 3.2.1)** (*31*). Importantly, no patient with exome sequencing data received radiotherapy following PLGG diagnosis.

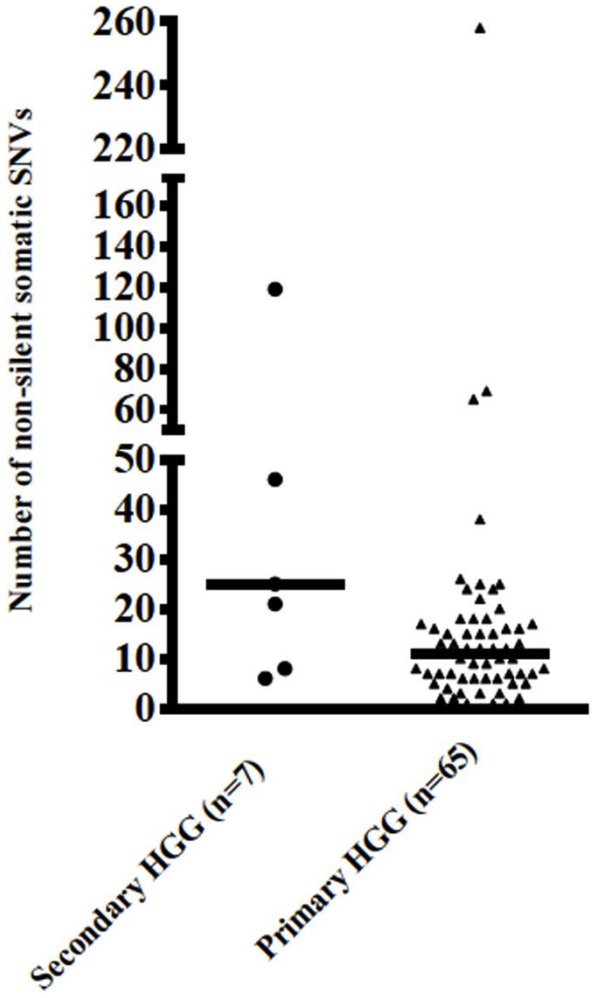

Figure 3.2.1: Somatic mutation load in secondary and primary high grade glioma. sHGG had a median of 25 somatic mutations (n=7), while pHGG harbored a median of 11 somatic mutations (n=65; p=0.0042). Each group had a single tumor showing a HPM phenotype (not shown).

3.2.2 Chromatin modifier and histone 3.3 variant analysis

Only one recurrent somatic point mutation was identified from exome-sequencing analysis, which is described in the next section. To uncover recurrently mutated pathways implicated in pediatric secondary high grade glioma, a prioritization scheme ranking chromatin modifier and histone variants was developed using exome data (**Appendix B**). Genes involved in histone 3.3 methylation pathway were used to develop the prioritization scheme and rank candidate variants as this pathway was previously implicated in pediatric primary high-grade glioma. Deep sequencing identified 4/7 (57%) patients with heterozygous missense mutations in chromatin modifying genes in their sHGG (**Table 3.2.2**), however only 1 mutation (*H3F3A* K27M) was validated using Sanger sequencing due to limited tissue availability. Additional targeted sequencing of all sHGG identified 19% (n=3/16) to harbor *H3F3A* K27M mutations, all located in the brainstem or thalamus (**Figure 3.4.1**).

Patient ID	Tumor ID	WHO Grade	Gene	Allele change	Amino acid change	Mutation type	WES	Sanger validated
16	D132	High	*SETD1B*	C>T	R1759C	Missense	Yes	No
19	D311	High	*H3F3A*	A>T	K27M	Missense	Yes	Yes
7	D154	High	*DOT1L*	C>A	R344S	Missense	Yes	No
20	D907	High	*DNMT1*	C>T	R139K	Missense	Yes	No

Table 3.2.2: Variants in chromatin modifier genes. 4 candidate variants in chromatin modifier genes were identified after prioritizing candidates. All variants were missense mutations predicted deleterious by polyphen-2 software and not identified in any publically available databases (NHLBI-ESP, CG, 1000 Genomes Project). 3/4 genes (excluding *DNMT1*) are involved with methylation of different lysine residues of histone 3.3.

3.2.3 Low frequency of IDH1 R132, H3F3A G34 and ATRX somatic mutations

Exome sequencing of 7sHGG did not identify any somatic mutations in IDH1 or H3F3A G34. Targeted mutation analysis of a cohort of 24 patients, including sHGG and matching PLGG which transform, for H3F3A G34 and IDH1 was also conducted to determine their frequency in the entire cohort. No PLGGs undergoing transformation had mutations in *H3F3A* G34 (0/13) or *IDH1* mutations (0/14) respectively. Sixteen sHGG were also sequenced for both alterations, also revealing no mutations (**Figure 3.4.1**). Only 1 of 7 sHGG harbored an *ATRX* stop-gain mutation (p.R1504*), which was identified in the HPM. The frequency of *ATRX* mutations was not validated as only 1 somatic mutation was identified from exome-sequencing analysis.

3.2.4 The BRAF V600E somatic point mutation is highly recurrent in sHGG

Remarkably, BRAF V600E (c.1799T>A) was found to be the most recurrent somatic non-silent point mutation, identified in 3/7 sHGG from the whole-exome sequencing cohort (43%). As this was the most recurrent somatic point mutation identified from the discovery cohort, we examined for this mutation in an overlapping, larger cohort of sHGG. Overall, the BRAF V600E mutation was identified, using Sanger sequencing and castPCR, in 39% (n=7/18) of sHGG (**Figure 3.4.1; Appendix C**)

3.3 Copy number alterations (CNA) in secondary high grade glioma

3.3.1 The rate of CNAs and recurrent copy number alterations using array-CGH

We interrogated 7 sHGG and 2 matching PLGG from the same 7 WES patients for recurrent CNAs using array-CGH and running the genomic segmentation algorithm. The CNA per sHGG genome was 100 (range 51 to 189), versus 56 (range, 51 to 60) in the 2 patient matched PLGG ($p=0.28$; student's unpaired T test).

Several important genes of interest were identified to have recurrent copy number changes. A recurrent focal copy number gain of 7p, which encompassed the *EGFR* gene, was identified in 3 of 7 cases. Two sHGG cases showed a region on 17q with heterozygous deletions, encompassing the *NF1* gene (#7 and #20). As expected, the patient previously diagnosed with LFS also showed a hemizygous deletion of 17p, which encompassed *TP53.* Both PLGGs harbored homozygous deletions of Xq21.1 (#16, 19), encompassing *ATRX*. However one tumor retained this homozygous deletion in their sHGG. This patient's sHGG also demonstrated a stop gain somatic mutation in *ATRX* (**Appendix D**).

3.3.2 9p21.3 (CDKN2A) chromosome deletion is the most recurrent copy number alteration in sHGG

The most recurrent CNA was a focal deletion of chromosome 9 (p21.3), encompassing the *CDKN2A* gene, occurring in 71% of patients from our discovery cohort (n=5/7). One of these cases was in the low-grade tumor of a patient, and not in the matching sHGG (patient #16). To determine the frequency of the *CDKN2A* gene deletion in the entire sHGG cohort, we performed real-time qPCR on 14 tumors, all from different patients. Overall, 57% (n=8/14) of sHGG had hemizygous or homozygous deletions of *CDKN2A* (**Figure 3.4.1; Appendix E**).

One of the 4 original deletions (hemizygous) in the sHGG identified through array-CGH did not validate using real-time qPCR (the sHGG from patient #18). Five of eight sHGG with available array data had homozygous deletions of *CDKN2A*, while the remaining 3 cases were heterozygous deletions. The four cases that were not deleted using array-CGH were confirmed to be balanced (copy number neutral) using real-time qPCR. Three of the sHGG with identified homozygous deletions using array-CGH were also confirmed to be homozygous deleted using the qPCR. As mentioned above, one sHGG with a hemizygous deletion did not successfully validate. Patient 16s PLGG was identified to have a deletion of this gene from array-CGH data, while their sHGG did not. This finding from array data was successfully validated using qPCR.

3.4 Integrative genetic, molecular and clinical analysis of childhood PLGG transformation

3.4.1 P53 and retinoblastoma (RB) pathway dysfunction

Notably, all but 1 patient (n=17/18) with genetic and molecular data for their sHGG did not receive RT following initial PLGG diagnosis, which suggests that these secondary tumors are not radiation-induced, and have a distinct disease etiology.

Thirteen of 18 (72%) sHGG demonstrated p53 dysfunction (defined as a sequencing mutation or overexpression of p53), in comparison to only 27% of PLGG (n=4/15), making p53 dysfunction more common following MT (p=0.0149; Fisher's exact test).

Abnormalities of the p53 and/or retinoblastoma tumor suppressor pathways (p53 dysfunction and/or *CDKN2A* deletions) were identified in 12 of 14 PLGG (86%) and 14 of 15 sHGG (93%). One of the two patients without abnormalities in either of these two pathways (#19) instead contained *H3F3A* K27M and *BRAF* V600E mutations in its PLGG and matched sHGG. Surprisingly, a high proportion of PLGG harbored these alterations, suggesting early ablation of cell cycle control in PLGG that later transform (**Figure 3.4.1**).

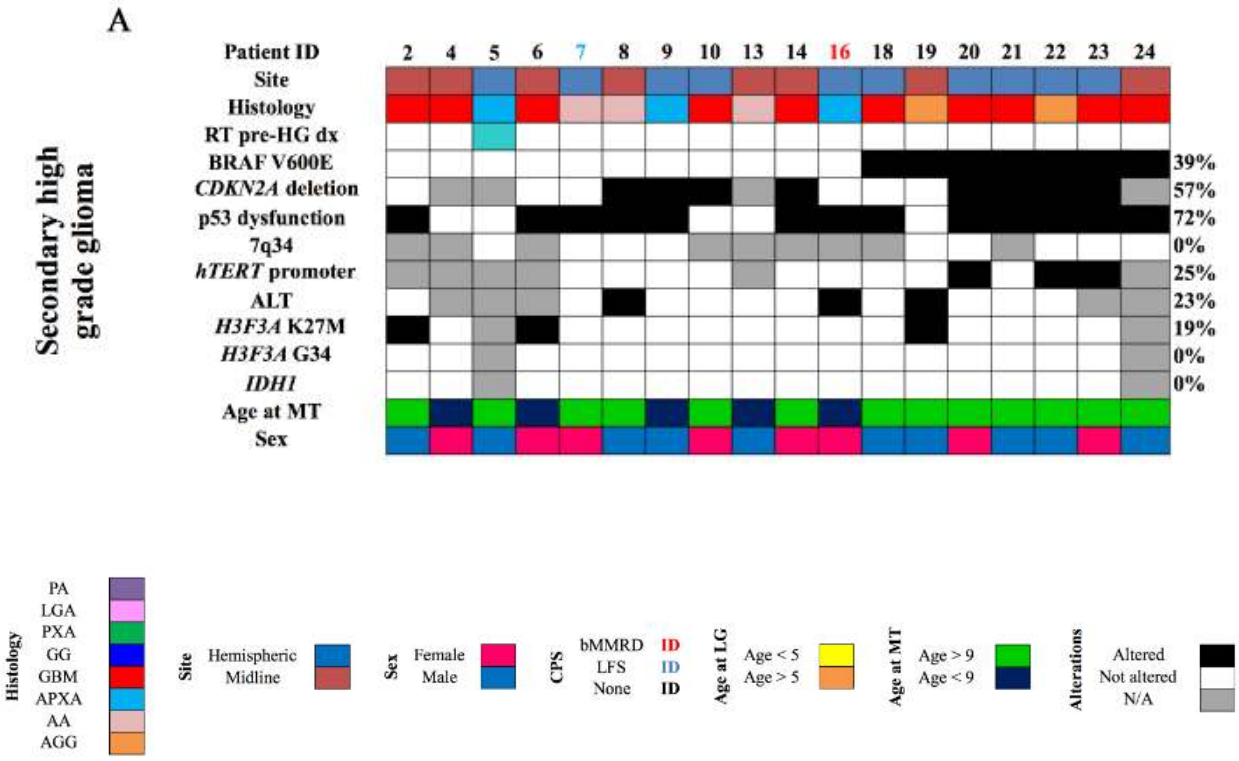

Figure 3.4.1. Genetic, molecular and clinical summary of (A) secondary high grade glioma. Incidence of alterations are noted in percentage. Black boxes represent a tumor is positive for an alteration. Gray boxes indicates insufficient tissue for analysis. White boxes indicate no alteration present. P53 dysfunction is defined by either 50% of immunopositive tumor cells for the p53 protein and/or *TP53* gene mutation. 7 patients with matched low and high grade samples are shown starting from the right.

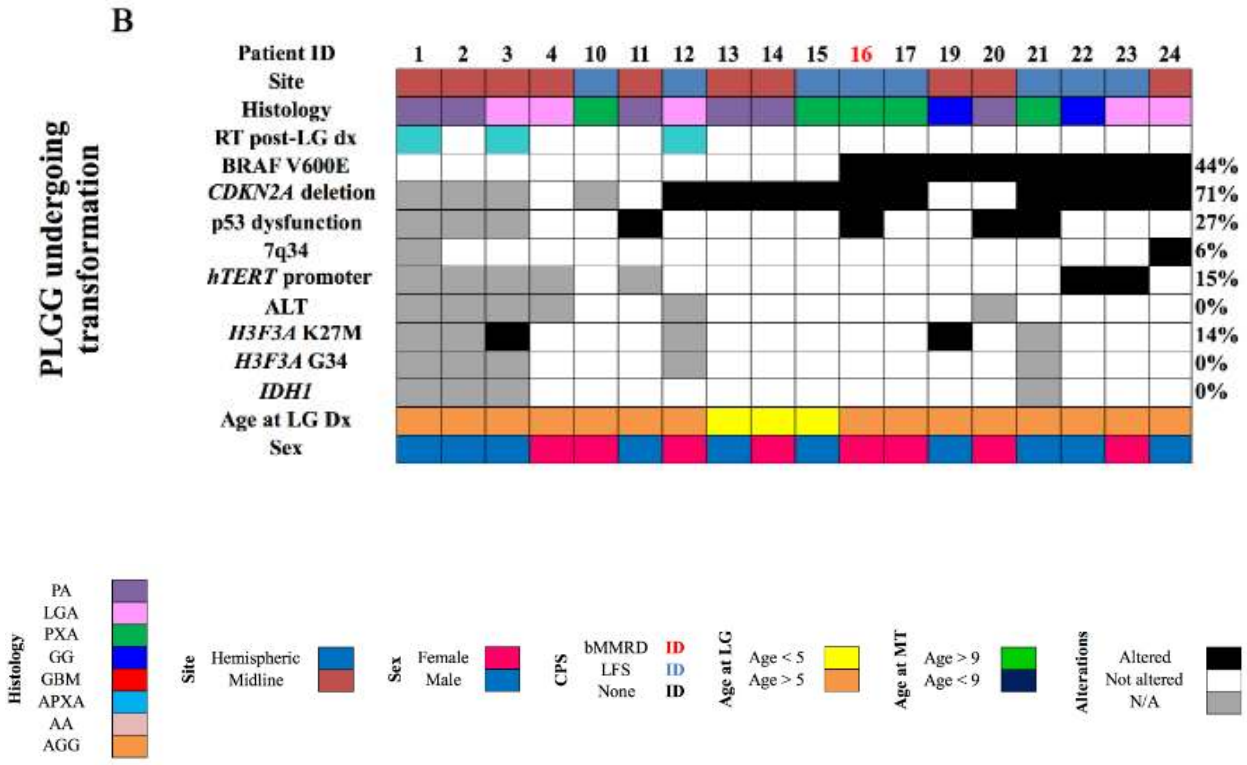

Figure 3.4.1. Genetic, molecular and clinical summary of (B) low grade glioma undergoing MT. Incidence of alterations are noted in percentage. Black boxes represent a tumor is positive for an alteration. Gray boxes indicates insufficient tissue for analysis. White boxes indicate no alteration present. P53 dysfunction is defined by either 50% of immunopositive tumor cells for the p53 protein and/or *TP53* gene mutation. 7 patients with matched low and high grade samples are shown starting from the right.

3.4.2 Clonal evolution of somatic point mutations in a patient-matched low and high grade glioma pair

Patient 16 harbored deleterious heterozygous *SETD1B* (p. R1759C) and *TP53* (p. R273C) missense mutations in their PLGG. These were the only 2 non-silent somatic point mutations out of 13 total mutations in the PLGG that were conserved to the HPM sHGG. Even more interestingly, both mutations increased in allelic fraction from low to high grade diagnoses. However, the BRAF V600E mutation identified originally in the low grade tumor at 9.09% allelic fraction was absent in the patient matched sHGG (**Table 3.4.2**).

The PLGG that demonstrated 7% TP53 mutant allelic fraction also demonstrated tumor cell immunopositivity for p53 (<25%). The matched sHGG tumor had a 30% mutant allelic percentage for the same mutation, with >90% of tumor cells staining positive for p53 (**Figure 3.4.2**). These observations suggest evidence of clonal evolution and selection for the *TP53* mutation during malignant transformation.

3.4.3 Low incidence of BRAF-KIAA1549 gene fusion

No sHGG harbored the 7q34 duplication, which is indicative of the oncogenic *BRAF-KIAA549* gene fusion (n=0/9) (*42, 73*). Notably, only 1 of the PLGGs that later transformed harbored that aberration (n=1/17; 6%). For this single case, the 7q34 duplication was identified in 10% of tumor cells examined and was not observed at all in the corresponding sHGG (**Figure 3.4.1**).

A

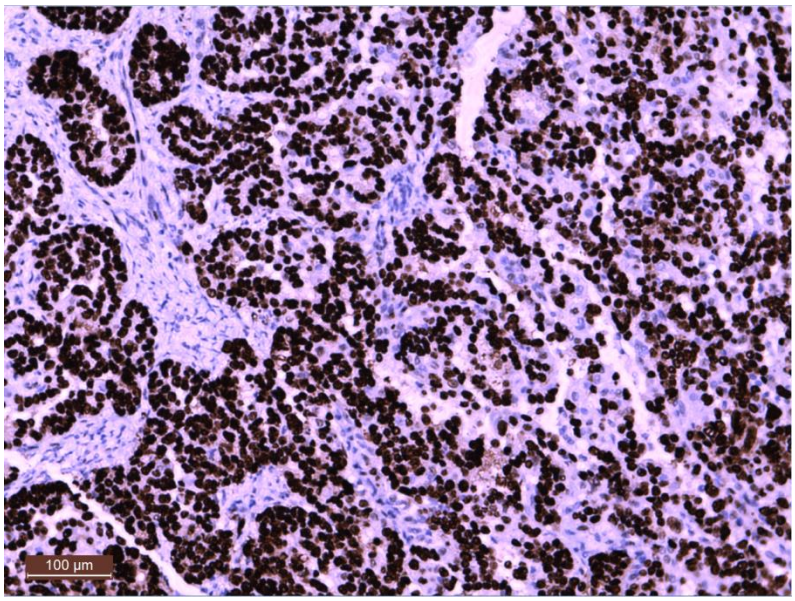

B

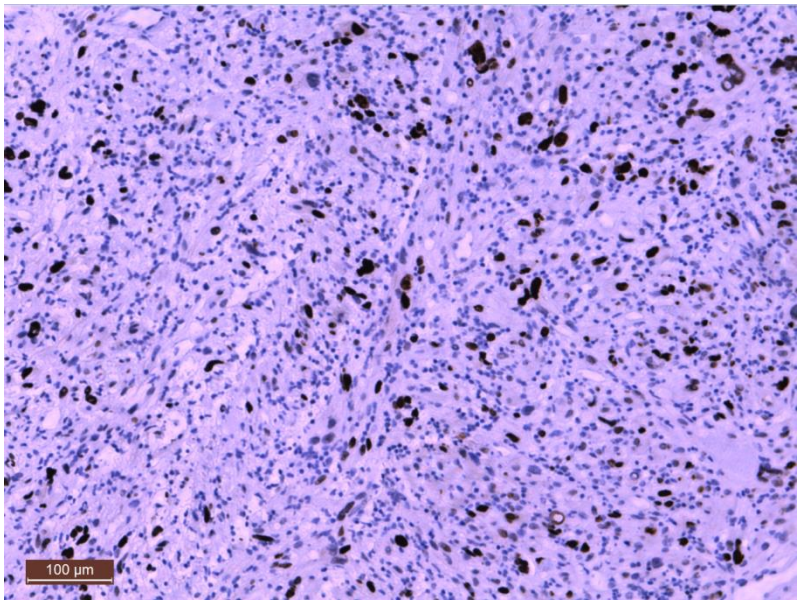

C

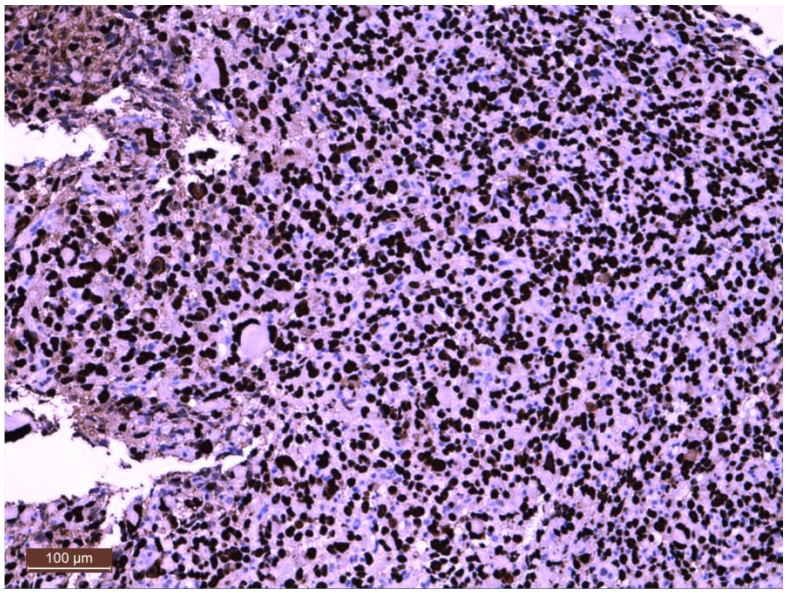

Figure 3.4.2: p53 immunostaining in (A) positive control tumor tissue with almost 100% of tumor cells staining for p53 (B) PLGG with 7% *TP53* mutant allelic fraction and <25% tumor cells staining positive p53 (C) and matching sHGG with 30% mutant allelic fraction with >90% p53 positive staining. 100x, magnification.

Patient ID	Tumor ID	WHO Grade	Gene	Allele change	Amino acid change	Mutation type	Mutant allelic fraction
16	D204	Low	*SETD1B*	C>T	R1759C	Missense	4%
	D132	High					38%
	D204	Low	*TP53*	C>T	R273C	Missense	7%
	D132	High					30%
	D204	Low	*BRAF*	T>A	V600E	Missense	9.09%
	D132	High					0%

Table 3.4.2: Allelic fraction of 3 missense mutations during malignant transformation of patient 16's PLGG. Missense mutations in *SETD1B* and *TP53* were the only 2 conserved to the matching sHGG, both of which increased in mutant allelic fraction. The *BRAF* V600E sub-clone of the PLGG was lost at transformation.

3.4.4 Telomere maintenance abnormalities are frequent in sHGG

Telomere maintenance abnormalities, specifically *hTERT* promoter mutations or alternative lengthening of telomeres (ALT) were investigated. Telomere abnormalities (either *hTERT* promoter mutation or ALT phenotype) existed in 54% of sHGG (n=7/13). No PLGG exhibited ALT (n=0/12). In contrast, Kannan et al. found that adult low grade glioma demonstrate the ALT phenotype at very high frequencies (43%; n=9/21) (*6*). *hTERT* promoter mutations were seen in 25% of sHGG (n=3/12) cases. Two of the 3 cases were found in matching PLGG counterparts (15%; n=2/13). The third case, patient (#20), acquired an *hTERT* promoter mutation at MT. All ALT and *hTERT* promoter mutations cases were mutually exclusive (**Figure 3.4.1**).

3.4.5 BRAF V600E and CDKN2A deletions are early genetic events in the transformation of pediatric low grade glioma

BRAF mutations and *CDKN2A* deletions define genetic subsets of sHGG, seen in 39% and 57% of cases respectively. To determine whether these alterations were early or late events in MT of PLGG, we investigated for their presence in patient matched PLGG. In 100% of cases, *BRAF* mutations identified in the sHGG were also identified in the patient matched PLGG (n=6/6 paired samples). In 80% of cases, *CDKN2A* deletions identified in the sHGG were also identified in the patient matched PLGG (n=4/5 paired samples) (**Figure 3.4.3**). Interestingly, 75% of BRAF V600E positive PLGGs also harbored concomitant *CDKN2A* deletions (n=6/8) (**Figure 3.4.1**).

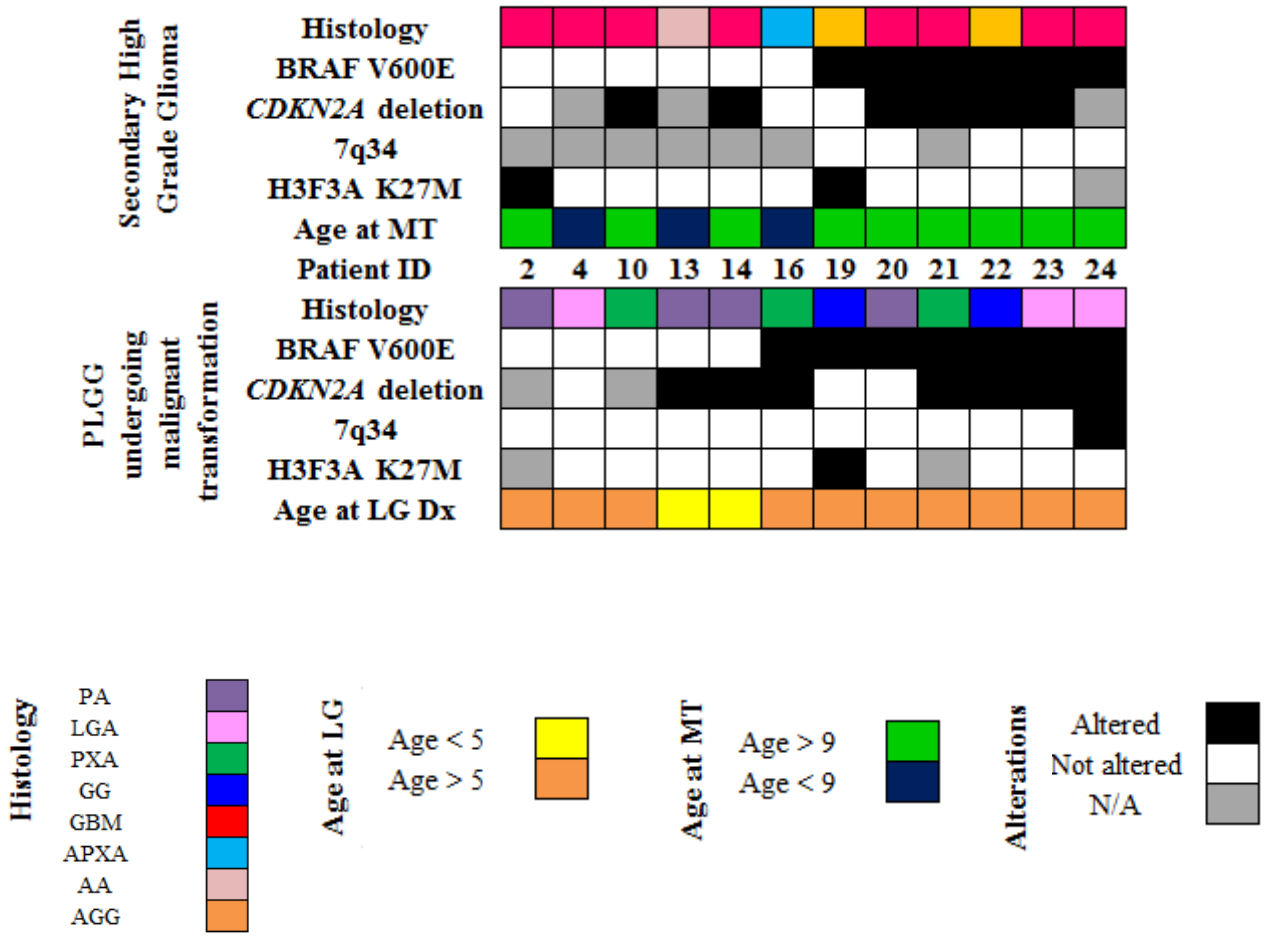

Figure 3.4.3: Genetic and genomic summarization of patients with matched low and high grade glioma pairs. 100% of BRAF V600E mutations in sHGG can be traced to matching low-grade counterparts, while 80% of *CDKN2A* deletions in sHGG can be traced back to matching low-grade counterparts. Low and high grade samples are matched for this figure. All BRAF V600E patients were above 9 years of age at high-grade diagnosis.

3.5 The genetic alterations unique to pediatric glioma that transform

To determine if oncogenic *BRAF* and *CDKN2A* deletions were unique to pediatric glioma undergoing transformation, we investigated for their presence in those tumors which did not transform. *BRAF* V600E was significantly enriched in 44% PLGG that transformed (n=8/18) in contrast to only 6% of those that did not (n=10/167; $p<0.0001$) (**Figure 3.5A**). These 167 cases were selected based on availability of BRAF mutation status. The mutation was also highly enriched in sHGG counterparts (n=7/18) as compared to only 1 of 31 pediatric primary HGG (**Figure 3.5B**; p=0.0023). Strikingly, this single patient had a 3-year history of headache and seizures prior to his diagnosis and is currently alive >15 years post-treatment for his sHGG. Similar to *BRAF*, *CDKN2A* deletions were significantly enriched for PLGG that transform (10/14), compared to those PLGG that did not (9/45) (**Figure 3.5C**; p=0.0007).

Of patients with available tissue for analysis, 88% (n=21/24) harbored aberrations in at least 1 of 4 well-characterized gliomagenesis pathways. In summary, these pathways (and their aberrations) include oncogenic MAPK (*BRAF* V600E), tumor suppressor pathways TP53 (p53 overexpression and/or loss of function mutations) and RB1 (*CDKN2A* deletions) and histone variant 3.3 tail methylation (*H3F3A* K27M).

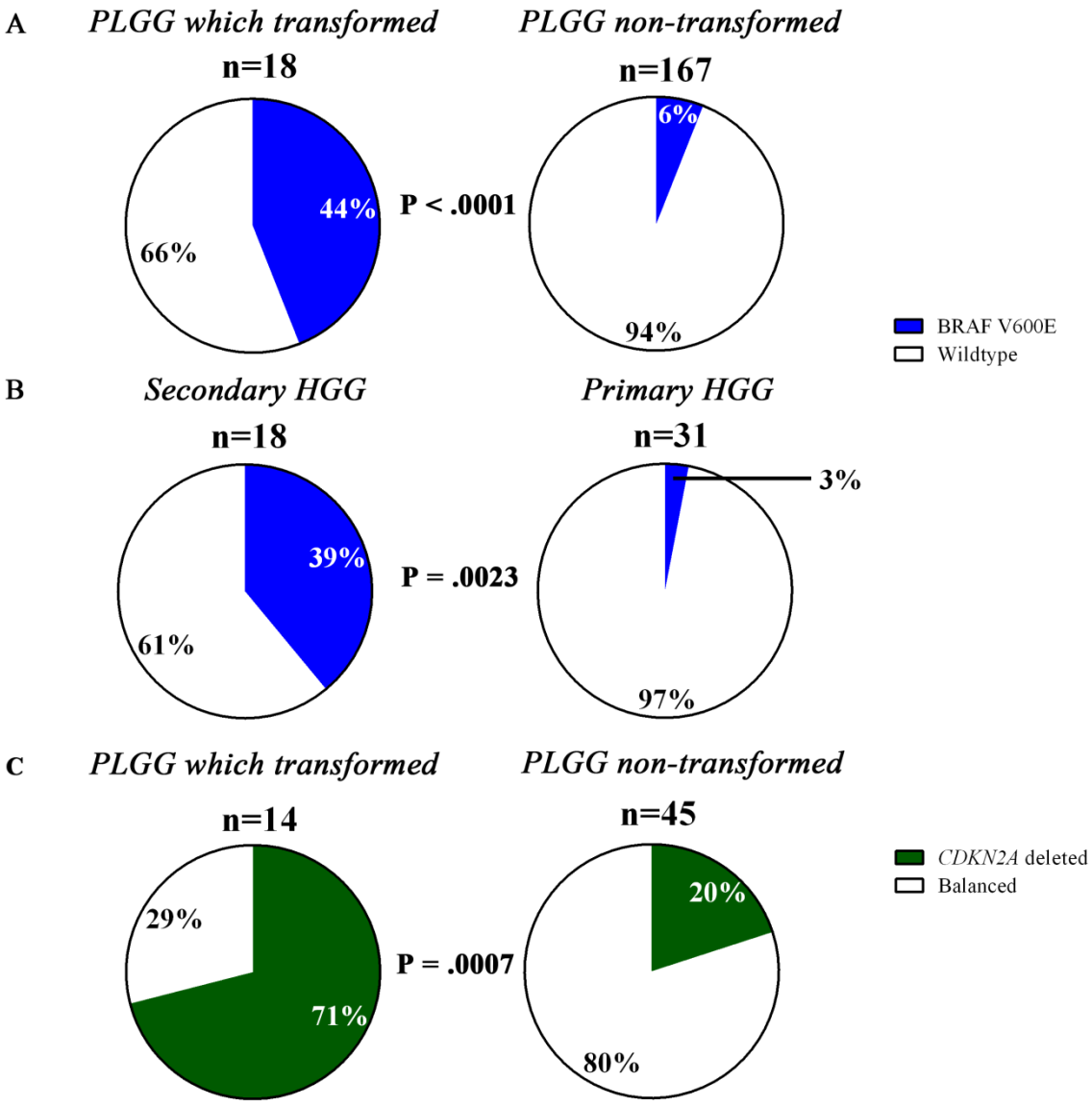

Figure 3.5: Frequency of BRAF V600E and CDKN2A deletions in pediatric glioma. (A) Incidence of the mutation in pediatric glioma undergoing MT (PLGG-MT) versus those which do not (PLGG) ($p<0.0001$). **(B)** Incidence of the mutation in sHGG versus pHGG ($p=0.0023$). **(C)** Incidence of the deletion in low grade glioma undergoing MT versus those which do not ($p=0.0007$).

3.6 Clinical outcome analysis based on BRAF V600E status

3.6.1 BRAF-mutant patients are diagnosed between 5 and 10 years of age

To understand the clinical consequences of the identified *BRAF* V600E driven sHGG subset, we compared onset and outcome of this subgroup to non-*BRAF* mutant sHGG. The median age at initial diagnosis between BRAF mutant and wild-type patients was very similar, being 7.26 (range, 5.1 to 13.4) and 5.75 years (range, 0.38 to 15.6) respectively (p=0.1584; unpaired student's T test). Interestingly, almost all *BRAF* mutant patients (89%; n=8/9) who experienced MT were diagnosed with PLGG between 5 and 10 years of age (**Figure 3.6.1**). Only one patient was diagnosed above 10 years old (range, 5.1 to 13.4 years).

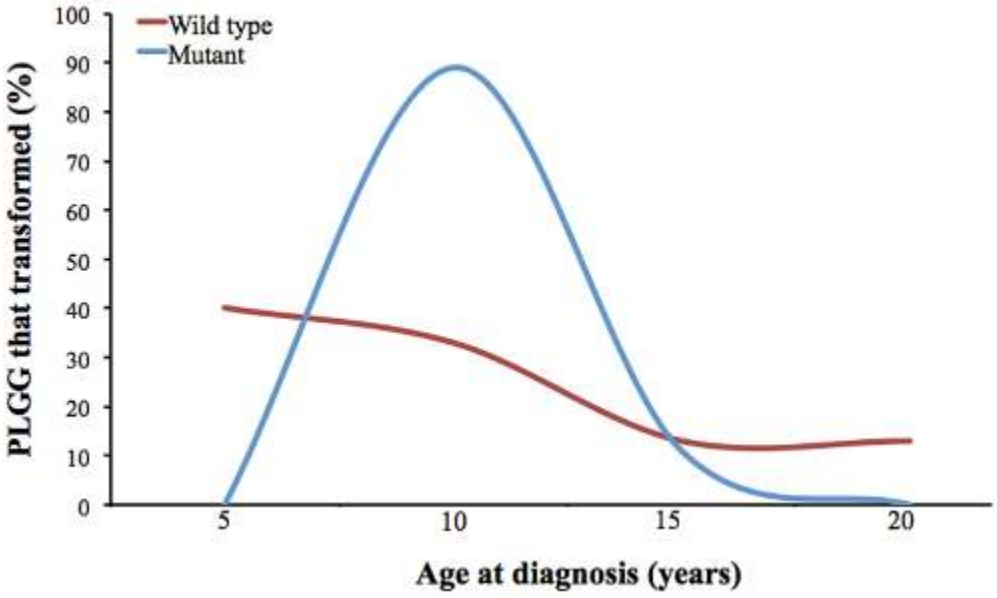

Figure 3.6.1: Age at PLGG diagnosis for BRAF mutant and wildtype patients. *BRAF* mutant patients have a median age of 7.26 years, similar to wildtype patients, who have a median age of 5.75 years at initial diagnosis. However all BRAF mutant patients were diagnosed above 5 years of age, with a 8/9 patients diagnosed between 5 and 10 years of age.

3.6.2 BRAF V600E PLGG have long latency periods to malignant transformation than BRAF-wildtype patients

The Ontario health system tracks patients for greater than 20 years, which allows for extended follow-up to identify very late transformation events. Most notably, PLGGs that transformed harboring the *BRAF* V600E mutation (n=8) demonstrate significantly prolonged latency periods to malignancy (median 6.65 years; range, 3.5 to 20.3 years) in comparison to *BRAF* wild-type PLGG (n=16) that also experience transformation (median 1.59 years; range, 0.32 to 15.9 years) (p=0.0389; unpaired student t test) (**Figure 3.6.2**). As a result, all *BRAF* mutant sHGG were diagnosed above 9 years of age (**Figure 3.2.3**).

We removed the single and only case which had a deeply-seeded PLGG with a short latency time (<1 year) to transformation, which may have resulted from biopsy bias. After doing so, the latency to transformation for PLGGs harboring BRAF V600E (n=8) was still prolonged in comparison to BRAF-wildtype patients (n=15), 6.65 years versus 1.62 years respectively (p=0.053).

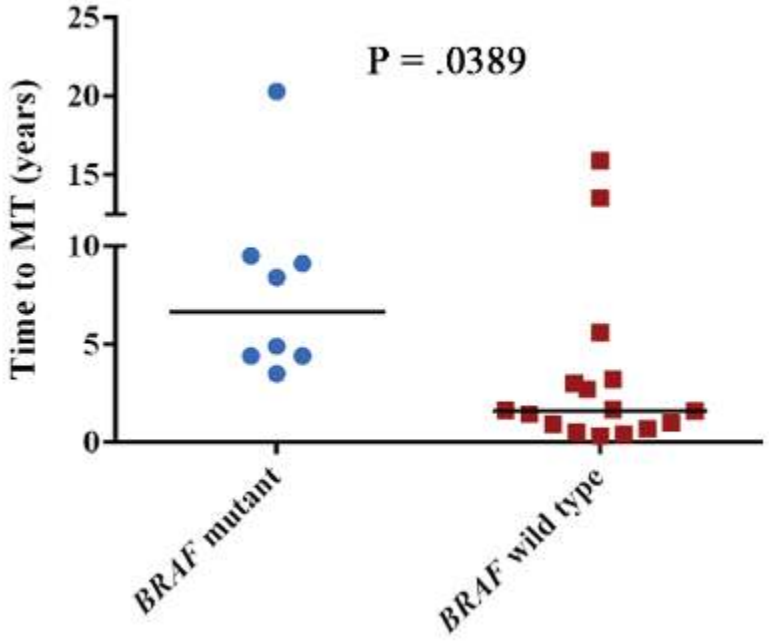

Figure 3.6.2: BRAF mutant patients have a prolonged period to malignant transformation. BRAF mutant patients (n=8) have a significantly longer latency period to MT (median 6.65 years) in comparison to all other patients (n=16) (median 1.59 years) (p=0.0389). Horizontal lines indicate medians.

3.6.3 BRAF V600E patients have better 5-year overall survival after diagnosis

BRAF mutant patients who experience transformation had a 5-year overall survival of 75% ± 15%, significantly better than *BRAF* wild-type patients (29% ± 12%) following PLGG diagnosis (p=0.024; **Figure 3.6.3A**).

Non-BRAF mutant sHGG have a better overall survival than primary HGG patients, which a 5-year overall survival of 5% ± 4% (p=0.0163). Non-transformed PLGG patients represent a very different disease as these patients have the best 5-year OS after initial diagnosis at 98% ± 0.5% (**Figure 3.6.3B**).

Following malignant transformation, 25/28 patients died and no significant difference in survival between subgroups of sHGG was observed. No difference in overall surivival was observed following malignant transformation between any high grade glioma group. BRAF-wildtype sHGG had an OS following MT diagnosis of 3.5% ± 5%, followed by 4.4% ± 4% for primary HGG, and finally 20% ± 15% for the *BRAF* mutant sHGG group (p=0.49; **Figure 3.6.3C**).

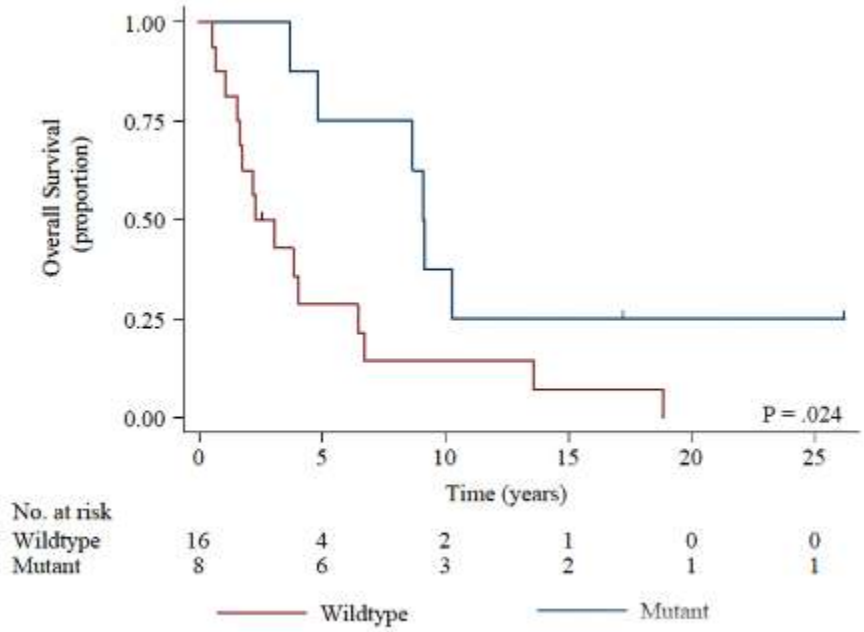

Figure 3.6.3. Overall survival following initial and MT diagnoses. **(A)** OS following initial diagnosis for pediatric glioma undergoing MT based on *BRAF* status. BRAF mutant PLGG have a better 5-year overall survival than all other PLGGs which transformed (wildtype).

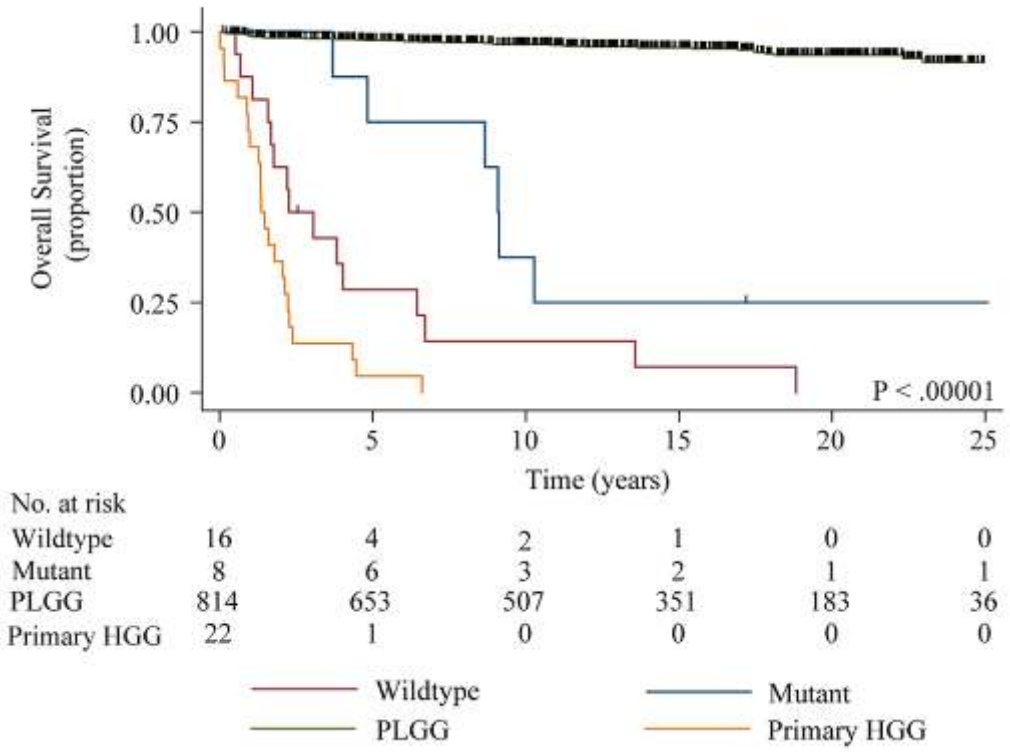

Figure 3.6.3. Overall survival following low and high diagnoses. **(B)** OS following initial diagnosis including pHGG and PLGG and pediatric glioma undergoing MT. Primary HGG had a worse overall survival than all pediatric gliomas. PLGGs had the best OS.

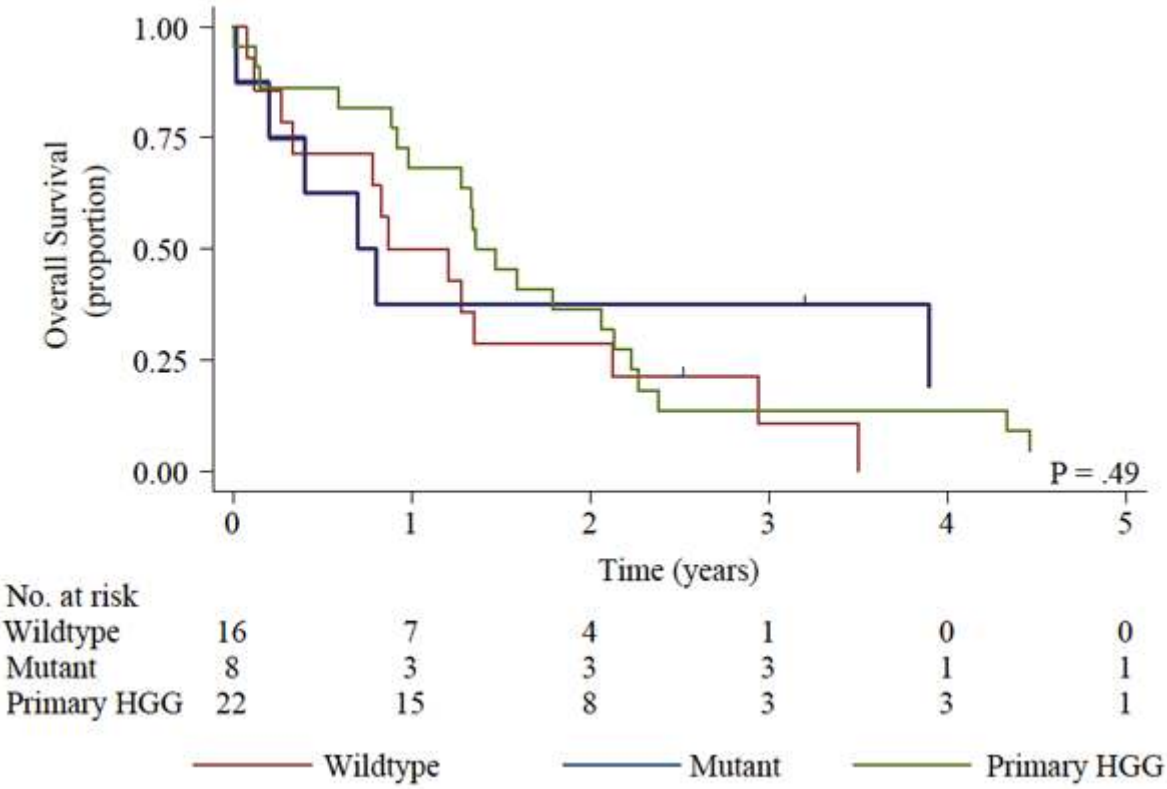

Figure 3.6.3. Overall survival following initial and MT diagnoses. **(C)** OS following low and high grade diagnosis between *BRAF* wildtype, mutant and all pHGG. There was no significant difference in survival when comparing any of these groups.

4 CHAPTER 4: DISCUSSION

The invariable tendency of adult low-grade glioma to undergo MT has facilitated the study and subsequent identification of several biological drivers of LGG transformation (*6*). In stark contrast, less than 10% of PLGG experience MT, which has limited the potential for discovery of prognostic biological markers to guide the clinical management and surveillance of this unique group (*33*). This thesis reports the risk of PLGG to transform to secondary high grade tumors and defines clinically applicable genetic subgroups of these cancers.

We found that the incidence of PLGG transformation is lower than previously reported, observed at 3.2% (*33*). This is probably due to lack of referrals in Ontario that enabled us to look at an unbiased population. Since referrals usually occur when tumors progress or transform, this may explain the lower rate of transformation in our cohort.

On the other hand, the provincial health care system and follow-up data allowed us to track patients for more than 30 years and detect even very late transformation events in survivors of PLGG. These late transformation events were not reported previously. Indeed, survivors of childhood *BRAF* mutant PLGG may experience malignant transformation up to 20 years following their initial diagnosis when they are well into adulthood.

Following exhaustive tissue collection from our institution, we compiled the largest transformation cohort to date. We use deep exonic sequencing, genotyping, copy number analyses and comprehensive clinical data to define a *BRAF* V600E subset of secondary high-grade glioma with concomitant *CDKN2A* deletions and early oncogenic *BRAF* as a prognostic marker for latent transformation.

Our study reveals additional molecular and genetic differences between childhood and adult gliomas. Whole-exome and targeted deep sequencing of adult low-grade glioma have identified *TP53*, *ATRX* and most notably, IDH mutations as critical drivers of LGG pathogenesis (*6*). Similarly, both PLGGs with available array data demonstrated homozygous deletions of *ATRX*. No *IDH1* mutations were observed in any PLGG in our cohort, yet 14% did harbor *H3F3A* K27M mutations (all thalamic or brainstem tumors), suggesting convergence between both groups towards aberrant methylation of lysine residues of H3.3 (*10, 74*). Previous reports observed only 1.9% of PLGGs to harbor K27M. The high frequency of K27M in our PLGG cohort warrants careful monitoring of the clinical course of midline K27M positive PLGGs as this mutation may suggest these tumors are indeed high-grade glioma (*45*).

Kannan and colleagues identified 34% (n=11/32) of their adult low-grade glioma to harbor *TP53* mutations (*6*). Similarly, 27% of our PLGGs that transformed demonstrated p53 dysfunction, suggesting aberrant p53 activity is a shared early event in glioma transformation in both the adults and children. P53 dysfunction was more common following MT, consistent with Broniscer *et al.* findings in their low-grade glioma cohort which experienced MT. Our larger cohort did provide the necessary power to achieve statistical significance, unlike in that study (*33*).

Interestingly, a small proportion of tumor cells showed p53 expression in patient 16's PLGG with only 4% *TP53* mutant allelic percentage, whereas this patients' malignant sHGG counterpart showed dense staining alongside a 30% mutant allelic percentage. These results suggest low allelic fraction *TP53* mutations may be identified at PLGG diagnosis via p53 immunopositive staining, and be suggestive of a more malignant pathology and aggressive clinical course, although this was only one such example. An important clinical implication of

this observation is the high incidence of both p53 positive immunostaining and *CDKN2A* deletion observed in the PLGG cohort. Since these 2 markers are extremely uncommon in PLGG, integration of these tests to the panel used at diagnosis may enable us to detect a high-risk patient population for follow-up.

Activation of telomere maintenance mechanisms appears to be essential for the immortalization of many human cancer cells. Two mechanisms, ALT and *hTERT* promoter mutations, are both observed in glioma. ALT was seen exclusively in our sHGG cases, but absent in PLGGs that went onto transform. In contrast, ALT is seen in 38% of adult LGG (*6*). Instead, several of our PLGGs harbored *hTERT* promoter mutations, which contrast the adult setting, where these mutations are observed only primary HGG.

The complete lack of the *BRAF-KIAA1549* gene fusion observed in sHGG represents another clinically important parameter for risk assessment. Out of our PLGG database of 888 patients, only one patient with chromosome 7q34 duplication went on to transform. This patient had only 10% of cells harboring this duplication and this clone disappeared in the corresponding sHGG. Since more than half of PLGG are expected to harbor this alteration, but only a single PLGG out of 888 at our center harbored this alteration, inclusion of this test will add important negative information on the risk of transformation (*37*).

The frequency of *BRAF* mutations in pediatric high-grade glioma is controversial. Different studies reveal rates between 10-25% (*10, 18, 56, 75*). This is the first study to use a genetic marker, the *BRAF* V600E mutation, to distinguish secondary from primary high-grade glioma in children. In fact, the single primary HGG patient with a *BRAF* mutation had a 3-year history of headache and seizures prior to diagnosis, however no MRI was conducted at presentation of these symptoms to suggest the presence of a low-grade lesion and this tumor may indeed

originated from a low grade lesion. Our observations resolve some of these discrepancies, as the mutation may be specific to a subgroup of sHGG rather than primary HGG.

Comparison of deep sequencing of sHGG from this study and primary HGG from Baker *et al*. suggests a higher somatic mutation frequency in the former group, perhaps due to accumulation of somatic mutations over time due to a longer clinical history of disease (*31*).

A previous study identified 5 of 7 pediatric astrocytoma (grades 2 to 4) to harbor oncogenic *BRAF* with *CDKN2A* inactivation (*18*). Moreover, Zhang *et al.* observed both alterations concurrently in 60% (6/10) of pediatric PXAs (*45*). Our study reveals childhood high-grade gliomas with *BRAF* V600E (with or without *CDKN2A* deletions) arise secondarily from low grade origins, arousing suspicion whether these similar genetic subsets from the previous groups may have experienced a similar clinical course to our own cohort (*18*).

Johnson *et al*. describe the loss of a *BRAF* V600E sub-clone from an initial adult glioma at recurrence, suggesting despite its proliferative advantage, sub-clonal drivers are not necessarily selected for or outcompete existing tumor clones. In our cohort, a *BRAF*-mutant sub-clone first identified a patients' PLGG (9% allelic fraction) was lost at transformation. Despite this single case however, 83% of our patients retained their *BRAF* mutation in their matched sHGG (*17, 31, 76*).

Perhaps the most important observation of this study is that specific alterations identified in sHGG could be traced to their PLGG counterparts, and that they are enriched in our transformed cohort. Both *BRAF* V600E and *CDKN2A* deleted tumors may be eligible for existing targeted therapies. If so, preventive measures including a more aggressive surgical approach and consideration of medical therapies, such as treatment with the BRAF V600E small molecule

inhibitor, even when a stable tumor is observed, may mitigate the devastating transformation event. Early intervention is especially important since the survival post-transformation of *BRAF* mutant sHGG does not differ from pediatric primary or *BRAF* wildtype secondary high grade glioma.

Although the *BRAF* mutation was significantly enriched in PLGG which transform, there was an over-representation of PXAs in comparison to the control group (21% versus 4% respectively). This is probably due to the inherent tendency of PXAs to undergo anaplastic changes in comparison to other histological subtypes. However, the frequency of the BRAF V600E mutation was virtually identical in both groups, suggesting that PXA histology, irrespective of mutation status, is an independent risk factor for anaplastic progression.

Wild-type *BRAF* sHGG could be divided into 2 groups. One includes midline lesions that are enriched for the *H3F3A* K27M mutations. This mutation can differentiate them from other brainstem PLGG that have excellent survival. The third group of sHGG includes patients with cancer predisposition syndromes. These patients may also benefit from surveillance and early intervention to prevent tumor transformation (*77, 78*).

Together, we observed alterations in 21/24 (88%) patients with PLGG that later transformed and no *BRAF* fusions in any secondary HGG. These genetic alterations could stratify PLGG into several risk groups (**Figure 4**): Tumors that have the *BRAF* fusion but lack the rest of the above alterations (excellent and long-term outcome and extremely low risk for transformation); PLGG harboring the BRAF V600E mutations and alterations in *CDKN2A* or *TP53* (higher risk for transformation and should be managed with care); PLGG originating with cancer predisposition syndromes associated with HGG (these tumors will eventually universally transform); and finally midline PLGG harboring H3.3 K27M mutations which will behave as primary HGG.

Since all these tests could be performed in most clinical laboratories, it may be worthwhile to add them to the current battery of tests used for PLGG.

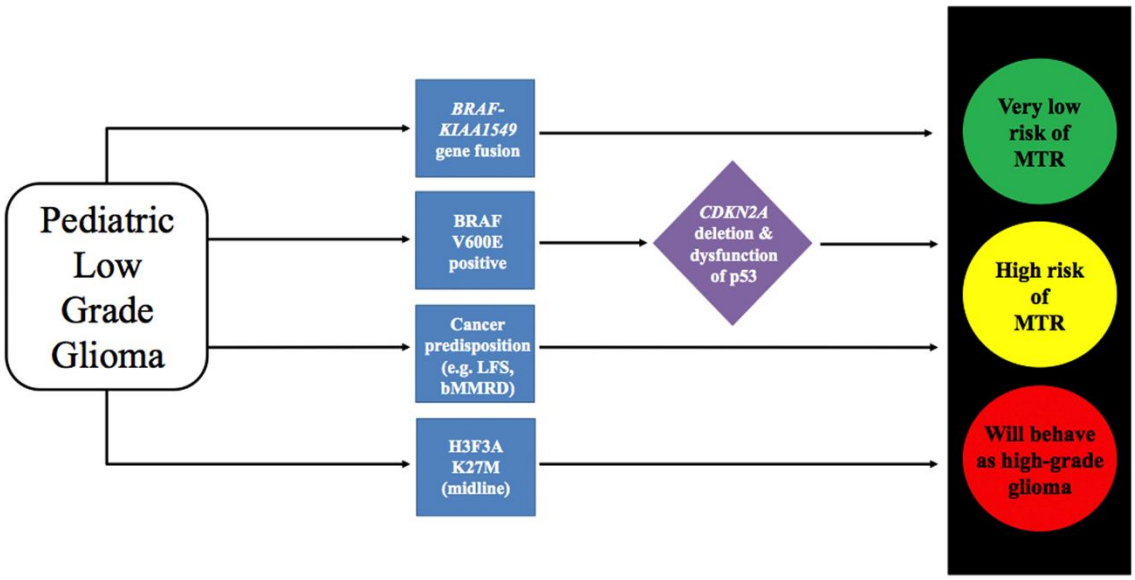

Figure 4: Stratification of PLGG into several risk groups. PLGG harboring the *BRAF-KIAA1549* fusion are at extremely low risk for transformation. BRAF V600E mutant PLGG cases are at high risk of transformation. PLGG from patients with cancer predisposition syndromes will eventually transform to sHGG. Midline PLGG that are H3F3A K27M positive behave as high-grade glioma. Abbreviations: MTR, malignant transformation.

We also acknowledge that some of the *BRAF* wild-type sHGG may actually represent primary HGG due to biopsy or surgical resection of low-grade portions of a tumor. This is especially true for deeply located tumors where a small biopsy may have missed malignant regions due to tumor heterogeneity. Indeed, 4 of our cases and previous reports (*33*) have identified midline low grade lesions followed by a second biopsy revealing high grade glioma in a short time span (less than 1 year). However, only 1 of these cases was included in the statistical analysis, as there was no available tissue on the other 3 cases to perform *BRAF* mutation analysis. After removing this case, *BRAF*-mutant patients still had much longer period to transformation than wildtype patients (median 6.65 years versus 1.62 years respectively).

Additionally, it is possible that tumors that behave clinically as high-grade in fact have low-grade histology. These cases have H3F3A K27M mutations which may explain their aggressive behavior (*79*). This further reinforces the combination of clinical, radiological and genetic findings in establishing the diagnosis of PLGG. Moreover, PLGGs that demonstrate mutations such as H3.3 K27M will behave more aggressive clinically, and should be treated high-grade glioma.

Importantly, *BRAF* status did not dictate significant differences in overall survival following high-grade diagnosis in our transformed cohort, suggesting the evolution of complex genomic landscape. Furthermore, no transformed patient with a BRAF mutation was treated with vemurafenib, the BRAF inhibitor, which may in fact change their survival. However, we do observe a significantly better 5-year overall survival for our *BRAF* mutant group early on following initial diagnosis. Our findings suggest patients with radiological evidence of PLGG between ages 5 to 10 should be strongly considered for biopsy (accessibility based) and undergo *BRAF* V600E mutation testing, regardless of histology, to qualify these patients for additional

gross surgery, targeted therapy with vemurafenib (BRAF V600E small molecule inhibitor) followed by extended and more frequent surveillance to mitigate the onset of latent MT. Further population-based research is required to better define the role of *BRAF* and *CDKN2A* alterations in childhood glioma.

5 CHAPTER 5: CONCLUSIONS

This study defines a new molecular and clinical entity in childhood brain tumors: secondary high-grade glioma. We defined the risk of transformation of pediatric low grade glioma in a population-based cohort using the unique set up in Ontario, Canada, in which a large population is treated at a single institution without referral bias and where excellent tissue banking and very long term follow-up (>30 years after diagnosis) are available for greater than 97% of patients.

We uncover the genetic and molecular characteristics of the previously uncharacterized secondary malignant counterparts of low-grade glioma in children using a discovery-based approach. We further traced two important genetic alterations in sHGG to their low-grade counterparts, and defined several important clinical parameters of this genetic subgroup of secondary high grade glioma.

Here, we identified the BRAF V600E mutation to distinguish secondary high-grade glioma from primary high grade glioma in children. Further, this oncogenic mutation was identified in patient-matched low grade glioma, alongside concurrent deletions of the *CDKN2A* gene. Importantly, these two alterations are unique to PLGG that later transform in comparison to those that do not. These findings validate the original hypothesis stating that secondary high grade glioma have a unique genetic landscape from primary high grade glioma, and some are indeed early events in the malignant transformation of PLGG.

Importantly, we show that *BRAF* V600E subgroup of secondary high-grade glioma have prolonged latency periods to transformation, and improved overall survival. Furthermore, we could detect specific genetic alterations (*BRAF* mutations, H3.3 mutations, *CDKN2A* deletions

and germline mutations in *TP53*, *NF1* and mismatch repair genes) in 88% (n=21/24) of children with secondary high-grade glioma.

These observations have important implications in the management of childhood low-grade gliomas since:

1) The most common alteration in childhood low-grade glioma (*BRAF-KIAA1549* gene fusion) was not detected in any of our transformed tumors suggesting that the majority of childhood PLGG with this alteration should be spared of aggressive therapies;

2) In contrast, tumors with *BRAF* mutations and *CDKN2A* deletions may benefit from early aggressive surgical intervention, targeted therapy with the BRAF inhibitor vemurafenib and implementation of extended surveillance. The long latency period of these cancers requires special consideration as these children enter adulthood to mitigate the devastating transformation event;

3) PLGG with *BRAF* mutations, H3.3 mutations, *CDKN2A* deletions or germline mutations in *TP53*, *NF1* or mismatch repair genes should be managed differently from the rest of childhood PLGG.

6 CHAPTER 6: FUTURE DIRECTIONS

Based on our findings, additional investigation into the association of BRAF V600E as a risk factor for pediatric low-grade glioma transformation using an independent validation cohort at another single referral institution is needed. Comparing clinical outcomes, including age at PLGG diagnosis, latency time to transformation and overall survival following initial diagnosis between *BRAF* mutant and wild-type patients should be studied in an independent cohort.

It would also be important to elucidate the role of *CDKN2A* deletions in PLGG transformation. In particular, a larger cohort of patients with PLGG is needed to identify the incidence of both the deletion and *BRAF* mutation in both PLGGs that transform versus those which do not to see if both alterations are concurrent risk factors for transformation. Due to the small cohort available for this study, we were unable to elucidate if the *CDKN2A* deleted subgroup had unique or different clinical features from the *BRAF* mutant subgroup. Using a larger, independent cohort, we could validate whether *BRAF* mutations and *CDKN2A* deletions are risk factors for transformation, determine if these two genetic alterations co-occur and finally, if they share similar clinical outcomes.

In vitro work using genetically similar pediatric glioma cell lines (BRAF V600E and *CDKN2A* deleted) and treating with existing FDA approved small molecule inhibitors vemurafenib (BRAF inhibitor) and nutlin-3 (p53 activator) would be an important next step following confirmation of both alterations concurrently predisposing PLGGs to transformation. Treating cell lines with each drug independently and then in combination to assess and attenuate cell proliferation, migration and viability.

Further investigation into the genetic and genomic features of *BRAF* wild-type PLGG that transform is also needed. Based on a small percentage of these patients from our cohort, mutations in histone H3.3 (H3F3A K27M) may play an important role in the early pathogenesis of malignant transformation of PLGG. A subset of the BRAF wild-type sHGGs consisted of patients with cancer predisposition syndromes, separately from K27M and V600E positive patients. As whole-exome sequencing and copy number analysis yielded little information about the genomic landscape of both of these groups in general, subgrouping based on RNA sequencing or global methylation arrays would be alternative discovery-based platforms to uncover predisposing features of BRAF wild-type PLGG that go onto transform.

From a clinical perspective, it would be important to assess how many PLGG patients at our center that did not transform that received radiotherapy, in comparison to those PLGG that did transform, to further elucidate the role radiation plays in transformation. A larger cohort would also be useful to determine if low grade glioma in particular anatomical locations of the brain are more likely to transform, and what treatment modality is typically given to patients with PLGGs in different parts of the central nervous system, and if predisposing alterations are location specific.

7 Appendices

7.1 Appendix A: Clinical characteristics and outcomes of pediatric low grade glioma patients which experience malignant transformation

Patient ID	Age at low grade dx (yrs)	Histological dx	Tumour location	Treatment for LGG	Age at high grade dx (yrs)	Latency to MT (yrs)	Histological dx at MT	OS after MT (yrs)
1	14.66	PA	Brainstem/pons	Chemo + RT + BX	16.33	1.67	N/A	0.10
2	6.81	PA	Brainstem/pons	Chemo + BX	10.63	2.96	GBM	0.87
3	5.17	PA	Brainstem/pons	Chemo + RT + BX	N/A	N/A	N/A	N/A
4	5.66	LGA	Brainstem/pons	None	7.81	1.62	GBM	0.12
5	15.58	LGA	Thalamus	RT + STR	18.30	2.74	AA	1.28
6	0.97	N/A	Brainstem/pons	None	6.58	5.61	AA	0.83
7	13.86	N/A	Frontal Lobe	None	17.06	3.20	AA	3.77
8	0.65	AG[T]	Thalamus	STR	16.54	15.89	AA	2.94
9	3.44	N/A	Left Parietal	STR	3.44	1.44	APXA	2.47
10	8.72	PXA	Frontal Lobe	Chemo + BX	9.72	1.00	APXA	1.21
11	12.81	PA	Thalamus	STR	13.22	0.41	AA	1.35
12	9.43	LGA	Cerebral Hemisphere	RT + STR	9.83	0.40	N/A	0.27

13	1.75	PA	Cerebellum	STR	2.04	0.29	AA	0.78
14	3.32	PA	Supracellar	Chemo + STR	16.81	13.49	GBM	0.08
15	0.39	PXA	Cerebral Hemisphere	Chemo + STR	0.57	0.18	APXA	0.34
16	5.84	PXA	Parietal-occipital	GTR	6.77	0.93	APXA	2.12
17	7.44	PXA	Cerebral Hemisphere	NTR	16.92	9.47	APXA	0.80
18	10.00	N/A	Temporal	None	14.42	4.42	GBM	0.40
19	5.63	GG	Thalamus	STR	9.11	3.48	AGG	0.21
20	5.06	PA	Suprachiasmatic	Chemo	14.13	9.07	GBM	0.02
21	7.08	PXA	Parietal Lobe	STR	11.47	4.39	GBM	21.71
22	9.60	GG	Temporal	STR	14.37	4.77	AGG	3.90
23	13.39	LGA	Left occipital	STR	33.71	20.32	GBM	3.20
24	6.11	LGA	Optic Pathway	Chemo + STR	14.53	8.42	AA	0.70
25	5.01	PA	Brainstem/pons	RT + BX	5.56	0.55	N/A	0.23
26	7.19	LGA	Thalamus	RT + BX + PR	7.62	0.44	N/A	0.83
27	15.33	LGA	Thalamus	Chemo + BX	16.04	0.71	AA	0.80
28	11.13	LGA	Thalamus	RT + STR	11.74	0.61	AA	0.11

Appendix A: Clinical Features and Treatment of Patients with Secondary High Grade Glioma. Abbreviations: PXA, pleomorphic xanthoastrocytoma; LGA, low grade astrocytoma; PA, pilocytic astrocyoma; AG, anaplastic glioma; PR, partial resection; NTR, non-total resection; Chemo, chemotherapy; STR, sub-total resection; RT, radiotherapy; BX, biopsy; GTR, gross total resection; APXA, anaplastic xanthoastrocyoma; GBM, glioblastoma; AA, anaplastic astrocytoma.

7.2 Appendix B: Somatic variant candidate prioritization scheme – histone 3.3 tail methylation pathway

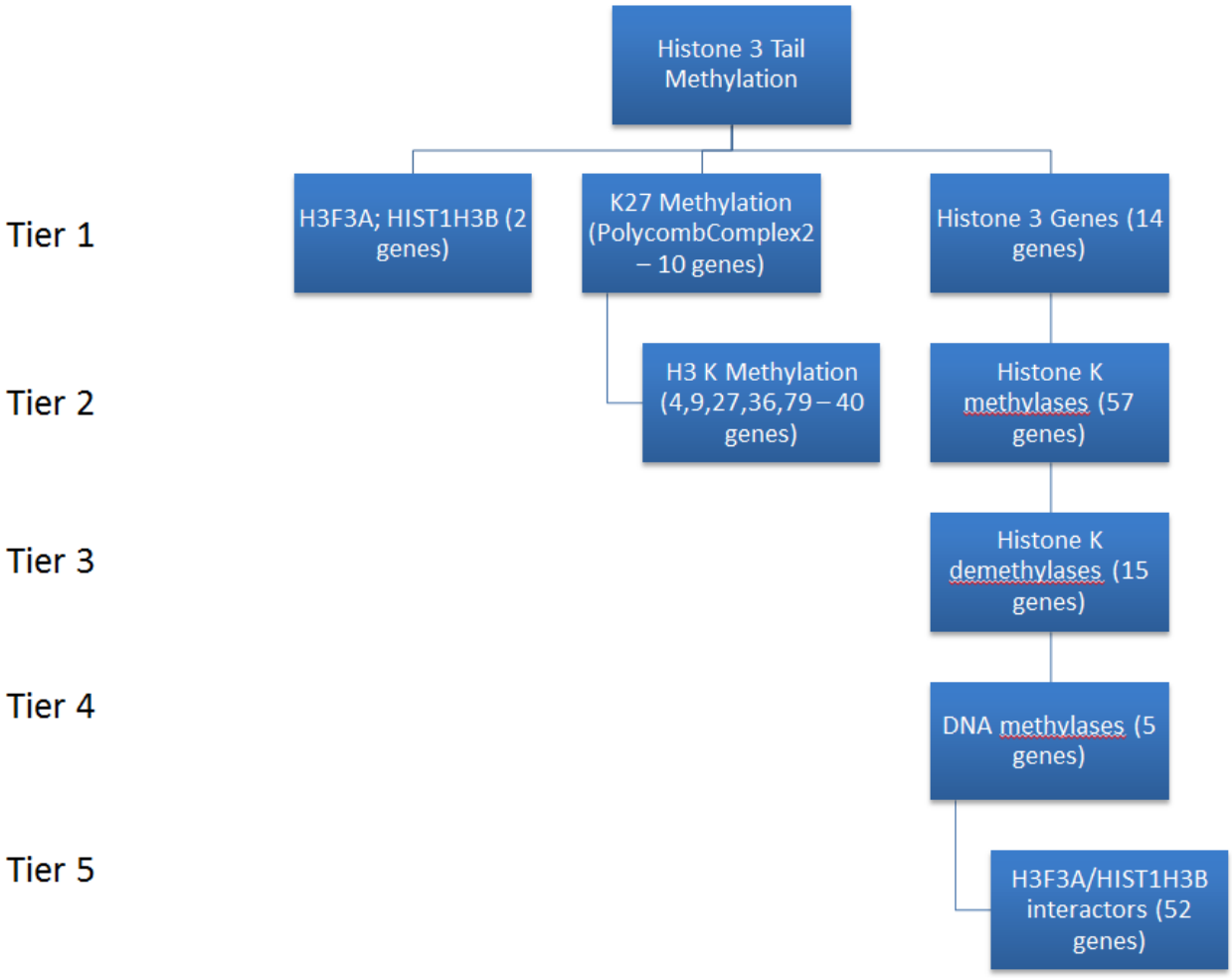

Appendix B: Candidate prioritization scheme for variant discovery. Variants from exome-sequencing data were ranked using a tier-structure to identify recurrent non-silent somatic mutations altering the methylation of lysine residues of histone 3.3 tail.

7.3 Appendix C: BRAF V600E genotyping across 3 platforms

Patient ID	WHO Grade	Histology	BRAF V600E - WES	BRAF V600E - Sanger	BRAF V600E - castPCR
1	Low	PA	N/A	N/A	0%
2	Low	PA	N/A	WT	N/A
3	Low	LGA	N/A	WT	N/A
4	Low	LGA	N/A	N/A	0%
	High	GBM	N/A	N/A	0%
5	High	AA	N/A	WT	N/A
6	High	GBM	N/A	WT	N/A
7	High	AA	WT	WT	0%
8	High	AA	WT	WT	0%
9	High	APXA	WT	WT	0%
10	Low	PXA	N/A	WT	0%
	High	APXA	N/A	WT	0%
11	Low	PA	N/A	WT	N/A
12	Low	LGA	N/A	WT	0%
13	Low	PA	N/A	WT	0%
	High	AA	N/A	WT	0%

14	Low	PA	N/A	WT	0%
	High	GBM	N/A	WT	N/A
15	Low	PXA	N/A	WT	0%
16	Low	PXA	HET	HET	9.09%
	High	APXA	WT	WT	0%
17	Low	PXA	N/A	HET	47.10%
18	High	GBM	HET	HET	16.30%
19	Low	GG	HET	HET	28.90%
	High	AGG	HET	HET	5.05%
20	Low	LGA	N/A	HET	26.90%
	High	GBM	HET	HET	35.70%
21	Low	PXA	N/A	HET	21.20%
	High	GBM	N/A	HET	77.20%
22	Low	GG	N/A	HET	N/A
	High	AGG	N/A	HET	N/A
23	Low	LGA	N/A	HET	N/A
	High	GBM	N/A	HET	N/A
24	Low	LGA	N/A	HET	56.70%
	High	GBM	N/A	HET	N/A

Appendix C: *BRAF* V600E genotyping across 3 platforms. BRAF mutation status in all sHGG and matching PLGG counterparts using whole-exome sequencing, Sanger sequencing and cast PCR.

7.4 Appendix D: Copy number alterations using array-CGH

Patient ID	Sample ID	WHO Grade	Gene Symbol	Chromosome	Length(bps)	# markers	Gain/loss
7	D154	High	*NF1*	chr17	5225545	252	HMZD
	D154	High	*TP53*	chr17	7823292	417	HMZD
	D154	High	*RB1*	chr13	14479137	641	HMZD
8	D417	High	*CDKN2A*	chr9	867543	38	HZD
	D417	High	*ATRX*	chrX	8732	4	High-level Amp
	D417	High	*PDGFRA*	chr4	98424944	4091	Amp
	D417	High	*MDM2*	chr12	34191545	1572	Amp
9	D848	High	*CDKN2A*	chr9	1250167	57	HZD
	D848	High	*ATRX*	chrX	8732	4	High-level Amp
16	D132	High	*ATRX*	chrX	8732	4	HZD
	D204	Low	*ATRX*	chrX	8732	4	HZD
	D204	Low	*CDKN2A*	chr9	6921931	289	HMZD
18	D909	High	*CDKN2A*	chr9	1877740	80	HMZD
	D909	High	*EGFR*	chr7	16867756	832	Amp
19	D26	Low	*ATRX*	chrX	3059	3	HZD

	D311	High	*EGFR*	chr7	29456562	1375	Amp
20	D907	High	*CDKN2A*	chr9	527087	26	HMZD
	D907	High	*ATRX*	chrX	74671415	6818	High-level Amp
	D907	High	*BRAF*	chr7	32895924	1833	High-level Amp
	D907	High	*NF1*	chr17	5303215	242	HMZD
	D907	High	*PTEN*	chr10	21638243	1471	HMZD
	D907	High	*EGFR*	chr7	79614633	3808	Amp

Appendix D: Copy number alterations of targeted gliomagenesis genes using array-CGH. The most recurrent CNA in sHGG was a focal deletion of chromosome 9 (9p21.3), encompassing the *CDKN2A*, a known tumor suppressor gene. It was observed in 71% of patients in total (n=5/7) from array-CGH data. Abbreviations: HMZD, hemizygous deletion; HZD, homozygous deletion; Amp, amplification; Chr, chromosome.

7.5 Appendix E*:* CDKN2A deletion incidence in sHGG and PLGG counterparts using real-time qPCR

Patient ID	Grade	Histology	9p21.3 deletion array-CGH	Chr.9:21994261 on NCBI build 37 (CDKN2A)	Chr.9:21967916 on NCBI build 37 (CDKN2A)
2	High	GBM	N/A	N/A	Balanced
4	Low	LGA	N/A	N/A	Balanced
6	High	GBM	N/A	N/A	Balanced
7	High	AA	Balanced	Balanced	Balanced
8	High	AA	Homozygous deletion	Homozygous deletion	Homozygous deletion
9	High	APXA	Homozygous deletion	N/A	Homozygous deletion
10	High	APXA	N/A	Hemizygous deletion	Hemizygous deletion
11	Low	PA	N/A	N/A	Balanced
12	Low	LGA	N/A	N/A	Hemizygous deletion
13	Low	LGA	N/A	N/A	Hemizygous deletion
14	Low	LGA	N/A	N/A	Hemizygous deletion

	High	GBM	N/A	N/A	Homozygous deletion
15	Low	PXA	N/A	N/A	Hemizygous deletion
16	Low	PXA	Homozygous deletion	Homozygous deletion	Homozygous deletion
	High	APXA	Balanced	Balanced	Balanced
17	Low	PXA	N/A	Homozygous deletion	Homozygous deletion
18	High	GBM	Hemizygous deletion	Balanced	Balanced
19	Low	GG	Balanced	Balanced	Balanced
	High	AGG	Balanced	Balanced	Balanced
20	Low	LGA	N/A	N/A	Balanced
	High	GBM	Hemizygous deletion	Hemizygous deletion	Hemizygous deletion
21	Low	PXA	N/A	N/A	Homozygous deletion
	High	GBM	N/A	N/A	Homozygous deletion
22	Low	GG	N/A	N/A	Hemizygous deletion
	High	AGG	N/A	N/A	Hemizygous

					deletion
23	Low	LGA	N/A	N/A	Homozygous deletion
	High	GBM	N/A	N/A	Homozygous deletion
24	Low	LGA	N/A	Homozygous deletion	Homozygous deletion

Appendix E*: CDKN2A* deletion incidence in sHGG and PLGG counterparts. Deletion status was obtained using real-time qPCR copy number assays. One region was in the 3'UTR of *CDKN2A*, while the second region (probe) was in exon 5 of *CDKN2A*. Abbreviations: HMZD, hemizygous deletion; HZD, homozygous deletion; GBM, glioblastoma; LGA, low grade astrocytoma; PXA, pleomorphic xanthroastrocytoma; GG, ganglioglioma; APXA, anaplastic pleomorphic xanthoastrocytoma; PA, pilocytic astrocytoma; AA, anaplastic astrocytoma; Balanced, copy number neutral. When sufficient DNA was available, both copy number assays for *CDKN2A* were in agreement.

References:

1. D. N. Louis *et al.*, The 2007 WHO classification of tumours of the central nervous system. *Acta neuropathologica* **114**, 97 (Aug, 2007).

2. C. Jones, L. Perryman, D. Hargrave, Paediatric and adult malignant glioma: close relatives or distant cousins? *Nature reviews. Clinical oncology* **9**, 400 (Jul, 2012).

3. F. B. Furnari *et al.*, Malignant astrocytic glioma: genetics, biology, and paths to treatment. *Genes & development* **21**, 2683 (Nov 1, 2007).

4. F. W. Huang *et al.*, Highly recurrent TERT promoter mutations in human melanoma. *Science (New York, N.Y.)* **339**, 957 (Feb 22, 2013).

5. P. Kleihues, H. Ohgaki, Primary and secondary glioblastomas: from concept to clinical diagnosis. *Neuro-oncology* **1**, 44 (Jan, 1999).

6. K. Kannan *et al.*, Whole-exome sequencing identifies ATRX mutation as a key molecular determinant in lower-grade glioma. *Oncotarget* **3**, 1194 (Oct, 2012).

7. Q. T. Ostrom *et al.*, CBTRUS statistical report: Primary brain and central nervous system tumors diagnosed in the United States in 2006-2010. *Neuro-oncology* **15 Suppl 2**, ii1 (Nov, 2013).

8. N. G. Gottardo, A. Gajjar, Chemotherapy for malignant brain tumors of childhood. *Journal of child neurology* **23**, 1149 (Oct, 2008).

9. T. F. Cloughesy, P. S. Mischel, New strategies in the molecular targeting of glioblastoma: how do you hit a moving target? *Clinical cancer research : an official journal of the American Association for Cancer Research* **17**, 6 (Jan 1, 2011).

10. J. Schwartzentruber *et al.*, Driver mutations in histone H3.3 and chromatin remodelling genes in paediatric glioblastoma. *Nature* **482**, 226 (Feb 9, 2012).

11. G. L. Gallia *et al.*, PIK3CA gene mutations in pediatric and adult glioblastoma multiforme. *Molecular cancer research : MCR* **4**, 709 (Oct, 2006).

12. E. W. Newcomb, M. Alonso, T. Sung, D. C. Miller, Incidence of p14ARF gene deletion in high-grade adult and pediatric astrocytomas. *Human pathology* **31**, 115 (Jan, 2000).

13. I. F. Pollack *et al.*, Age and TP53 mutation frequency in childhood malignant gliomas: results in a multi-institutional cohort. *Cancer research* **61**, 7404 (Oct 15, 2001).

14. D. Faury *et al.*, Molecular profiling identifies prognostic subgroups of pediatric glioblastoma and shows increased YB-1 expression in tumors. *Journal of clinical oncology : official journal of the American Society of Clinical Oncology* **25**, 1196 (Apr 1, 2007).

15. H. Q. Qu *et al.*, Genome-wide profiling using single-nucleotide polymorphism arrays identifies novel chromosomal imbalances in pediatric glioblastomas. *Neuro-oncology* **12**, 153 (Feb, 2010).

16. B. S. Paugh *et al.*, Genome-wide analyses identify recurrent amplifications of receptor tyrosine kinases and cell-cycle regulatory genes in diffuse intrinsic pontine glioma. *Journal of clinical oncology : official journal of the American Society of Clinical Oncology* **29**, 3999 (Oct 20, 2011).

17. B. S. Paugh *et al.*, Integrated molecular genetic profiling of pediatric high-grade gliomas reveals key differences with the adult disease. *Journal of clinical oncology : official journal of the American Society of Clinical Oncology* **28**, 3061 (Jun 20, 2010).

18. J. D. Schiffman *et al.*, Oncogenic BRAF mutation with CDKN2A inactivation is characteristic of a subset of pediatric malignant astrocytomas. *Cancer research* **70**, 512 (Jan 15, 2010).

19. S. Puget *et al.*, Mesenchymal transition and PDGFRA amplification/mutation are key distinct oncogenic events in pediatric diffuse intrinsic pontine gliomas. *PloS one* **7**, e30313 (2012).

20. M. Zarghooni *et al.*, Whole-genome profiling of pediatric diffuse intrinsic pontine gliomas highlights platelet-derived growth factor receptor alpha and poly (ADP-ribose) polymerase as potential therapeutic targets. *Journal of clinical oncology : official journal of the American Society of Clinical Oncology* **28**, 1337 (Mar 10, 2010).

21. D. W. Parsons *et al.*, An integrated genomic analysis of human glioblastoma multiforme. *Science (New York, N.Y.)* **321**, 1807 (Sep 26, 2008).

22. Comprehensive genomic characterization defines human glioblastoma genes and core pathways. *Nature* **455**, 1061 (Oct 23, 2008).

23. D. A. Bax *et al.*, A distinct spectrum of copy number aberrations in pediatric high-grade gliomas. *Clinical cancer research : an official journal of the American Association for Cancer Research* **16**, 3368 (Jul 1, 2010).

24. J. Barrow *et al.*, Homozygous loss of ADAM3A revealed by genome-wide analysis of pediatric high-grade glioma and diffuse intrinsic pontine gliomas. *Neuro-oncology* **13**, 212 (Feb, 2011).

25. P. Buczkowicz *et al.*, Genomic analysis of diffuse intrinsic pontine gliomas identifies three molecular subgroups and recurrent activating ACVR1 mutations. *Nature genetics* **46**, 451 (May, 2014).

26. G. Wu *et al.*, Somatic histone H3 alterations in pediatric diffuse intrinsic pontine gliomas and non-brainstem glioblastomas. *Nature genetics* **44**, 251 (Mar, 2012).

27. D. A. Khuong-Quang *et al.*, K27M mutation in histone H3.3 defines clinically and biologically distinct subgroups of pediatric diffuse intrinsic pontine gliomas. *Acta neuropathologica* **124**, 439 (Sep, 2012).

28. D. Sturm *et al.*, Hotspot mutations in H3F3A and IDH1 define distinct epigenetic and biological subgroups of glioblastoma. *Cancer cell* **22**, 425 (Oct 16, 2012).

29. A. M. Fontebasso *et al.*, Mutations in SETD2 and genes affecting histone H3K36 methylation target hemispheric high-grade gliomas. *Acta neuropathologica* **125**, 659 (May, 2013).

30. M. Antonelli *et al.*, Prognostic significance of histological grading, p53 status, YKL-40 expression, and IDH1 mutations in pediatric high-grade gliomas. *Journal of neuro-oncology* **99**, 209 (Sep, 2010).

31. G. Wu *et al.*, The genomic landscape of diffuse intrinsic pontine glioma and pediatric non-brainstem high-grade glioma. *Nature genetics* **46**, 444 (May, 2014).

32. P. J. Killela *et al.*, TERT promoter mutations occur frequently in gliomas and a subset of tumors derived from cells with low rates of self-renewal. *Proceedings of the National Academy of Sciences of the United States of America* **110**, 6021 (Apr 9, 2013).

33. A. Broniscer *et al.*, Clinical and molecular characteristics of malignant transformation of low-grade glioma in children. *Journal of clinical oncology : official journal of the American Society of Clinical Oncology* **25**, 682 (Feb 20, 2007).

34. G. T. Armstrong *et al.*, Survival and long-term health and cognitive outcomes after low-grade glioma. *Neuro-oncology* **13**, 223 (Feb, 2011).

35. R. S. Arora *et al.*, Age-incidence patterns of primary CNS tumors in children, adolescents, and adults in England. *Neuro-oncology* **11**, 403 (Aug, 2009).

36. I. Qaddoumi, I. Sultan, A. Gajjar, Outcome and prognostic features in pediatric gliomas: a review of 6212 cases from the Surveillance, Epidemiology, and End Results database. *Cancer* **115**, 5761 (Dec 15, 2009).

37. C. Hawkins *et al.*, BRAF-KIAA1549 fusion predicts better clinical outcome in pediatric low-grade astrocytoma. *Clinical cancer research : an official journal of the American Association for Cancer Research* **17**, 4790 (Jul 15, 2011).

38. A. Gajjar *et al.*, Low-grade astrocytoma: a decade of experience at St. Jude Children's Research Hospital. *Journal of clinical oncology : official journal of the American Society of Clinical Oncology* **15**, 2792 (Aug, 1997).

39. S. Yunoue *et al.*, Neurofibromatosis type I tumor suppressor neurofibromin regulates neuronal differentiation via its GTPase-activating protein function toward Ras. *The Journal of biological chemistry* **278**, 26958 (Jul 18, 2003).

40. S. Pfister *et al.*, BRAF gene duplication constitutes a mechanism of MAPK pathway activation in low-grade astrocytomas. *The Journal of clinical investigation* **118**, 1739 (May, 2008).

41. R. G. Tatevossian *et al.*, MAPK pathway activation and the origins of pediatric low-grade astrocytomas. *Journal of cellular physiology* **222**, 509 (Mar, 2010).

42. D. T. Jones *et al.*, Tandem duplication producing a novel oncogenic BRAF fusion gene defines the majority of pilocytic astrocytomas. *Cancer research* **68**, 8673 (Nov 1, 2008).

43. C. Michaloglou *et al.*, BRAFE600-associated senescence-like cell cycle arrest of human naevi. *Nature* **436**, 720 (Aug 4, 2005).

44. E. H. Raabe *et al.*, BRAF activation induces transformation and then senescence in human neural stem cells: a pilocytic astrocytoma model. *Clinical cancer research : an official journal of the American Association for Cancer Research* **17**, 3590 (Jun 1, 2011).

45. J. Zhang *et al.*, Whole-genome sequencing identifies genetic alterations in pediatric low-grade gliomas. *Nature genetics* **45**, 602 (Jun, 2013).

46. M. J. Garnett, R. Marais, Guilty as charged: B-RAF is a human oncogene. *Cancer cell* **6**, 313 (Oct, 2004).

47. H. Davies *et al.*, Mutations of the BRAF gene in human cancer. *Nature* **417**, 949 (Jun 27, 2002).

48. C. Michaloglou, L. C. Vredeveld, W. J. Mooi, D. S. Peeper, BRAF(E600) in benign and malignant human tumours. *Oncogene* **27**, 877 (Feb 7, 2008).

49. A. Tannapfel *et al.*, Mutations of the BRAF gene in cholangiocarcinoma but not in hepatocellular carcinoma. *Gut* **52**, 706 (May, 2003).

50. E. R. Cantwell-Dorris, J. J. O'Leary, O. M. Sheils, BRAFV600E: implications for carcinogenesis and molecular therapy. *Molecular cancer therapeutics* **10**, 385 (Mar, 2011).

51. G. Schindler *et al.*, Analysis of BRAF V600E mutation in 1,320 nervous system tumors reveals high mutation frequencies in pleomorphic xanthoastrocytoma, ganglioglioma and extra-cerebellar pilocytic astrocytoma. *Acta neuropathologica* **121**, 397 (Mar, 2011).

52. C. Koelsche *et al.*, Mutant BRAF V600E protein in ganglioglioma is predominantly expressed by neuronal tumor cells. *Acta neuropathologica* **125**, 891 (Jun, 2013).

53. S. Dahiya *et al.*, BRAF(V600E) mutation is a negative prognosticator in pediatric ganglioglioma. *Acta neuropathologica* **125**, 901 (Jun, 2013).

54. D. Dias-Santagata *et al.*, BRAF V600E mutations are common in pleomorphic xanthoastrocytoma: diagnostic and therapeutic implications. *PloS one* **6**, e17948 (2011).

55. P. B. Chapman *et al.*, Improved survival with vemurafenib in melanoma with BRAF V600E mutation. *The New England journal of medicine* **364**, 2507 (Jun 30, 2011).

56. T. P. Nicolaides *et al.*, Targeted therapy for BRAFV600E malignant astrocytoma. *Clinical cancer research : an official journal of the American Association for Cancer Research* **17**, 7595 (Dec 15, 2011).

57. R. G. Weber *et al.*, Frequent loss of chromosome 9, homozygous CDKN2A/p14(ARF)/CDKN2B deletion and low TSC1 mRNA expression in pleomorphic xanthoastrocytomas. *Oncogene* **26**, 1088 (Feb 15, 2007).

58. X. H. Pei, Y. Xiong, Biochemical and cellular mechanisms of mammalian CDK inhibitors: a few unresolved issues. *Oncogene* **24**, 2787 (Apr 18, 2005).

59. P. B. Dirks *et al.*, Development of anaplastic changes in low-grade astrocytomas of childhood. *Neurosurgery* **34**, 68 (Jan, 1994).

60. M. D. Krieger, I. Gonzalez-Gomez, M. L. Levy, J. G. McComb, Recurrence patterns and anaplastic change in a long-term study of pilocytic astrocytomas. *Pediatric neurosurgery* **27**, 1 (Jul, 1997).

61. A. J. Huttner *et al.*, Clinicopathologic study of glioblastoma in children with neurofibromatosis type 1. *Pediatric blood & cancer* **54**, 890 (Jul 1, 2010).

62. S. Sharif *et al.*, Second primary tumors in neurofibromatosis 1 patients treated for optic glioma: substantial risks after radiotherapy. *Journal of clinical oncology : official journal of the American Society of Clinical Oncology* **24**, 2570 (Jun 1, 2006).

63. S. L. Harris, A. J. Levine, The p53 pathway: positive and negative feedback loops. *Oncogene* **24**, 2899 (Apr 18, 2005).

64. I. Fried *et al.*, Favorable outcome with conservative treatment for children with low grade brainstem tumors. *Pediatric blood & cancer* **58**, 556 (Apr, 2012).

65. E. C. Torchia, K. Boyd, J. E. Rehg, C. Qu, S. J. Baker, EWS/FLI-1 induces rapid onset of myeloid/erythroid leukemia in mice. *Molecular and cellular biology* **27**, 7918 (Nov, 2007).

66. K. Cibulskis *et al.*, Sensitive detection of somatic point mutations in impure and heterogeneous cancer samples. *Nature biotechnology* **31**, 213 (Mar, 2013).

67. S. P. Cheng *et al.*, Significance of Allelic Percentage of BRAF c.1799T > A (V600E) Mutation in Papillary Thyroid Carcinoma. *Annals of surgical oncology*, (Apr 19, 2014).

68. M. Remke *et al.*, TERT promoter mutations are highly recurrent in SHH subgroup medulloblastoma. *Acta neuropathologica* **126**, 917 (Dec, 2013).

69. P. Berggren *et al.*, Detecting homozygous deletions in the CDKN2A(p16(INK4a))/ARF(p14(ARF)) gene in urinary bladder cancer using real-time

quantitative PCR. *Clinical cancer research : an official journal of the American Association for Cancer Research* **9**, 235 (Jan, 2003).

70. I. F. Pollack *et al.*, Expression of p53 and prognosis in children with malignant gliomas. *The New England journal of medicine* **346**, 420 (Feb 7, 2002).

71. C. Y. Henson JD, Huschtscha LI, Chang AC, Au AYM, Pickett HA and Reddel RR, DNA C-circles are specific and quantifiable markers of alternative-lengthening-of-telomeres activity. *Nature Biotechnology* **27**, 1181 (2009).

72. D. R. Lau LMS, Henson JD, Au AYM, Royds JA, Reddel RR, Detection of alternative lengthening of telomeres by telomere quantitative PCR. *Nucleic Acids Research* **41**, (2013).

73. A. J. Sievert *et al.*, Duplication of 7q34 in pediatric low-grade astrocytomas detected by high-density single-nucleotide polymorphism-based genotype arrays results in a novel BRAF fusion gene. *Brain pathology (Zurich, Switzerland)* **19**, 449 (Jul, 2009).

74. L. Dang *et al.*, Cancer-associated IDH1 mutations produce 2-hydroxyglutarate. *Nature* **465**, 966 (Jun 17, 2010).

75. C. W. Brennan *et al.*, The somatic genomic landscape of glioblastoma. *Cell* **155**, 462 (Oct 10, 2013).

76. B. E. Johnson *et al.*, Mutational analysis reveals the origin and therapy-driven evolution of recurrent glioma. *Science (New York, N.Y.)* **343**, 189 (Jan 10, 2014).

77. D. Bakry *et al.*, Genetic and clinical determinants of constitutional mismatch repair deficiency syndrome: report from the constitutional mismatch repair deficiency consortium. *European journal of cancer (Oxford, England : 1990)* **50**, 987 (Mar, 2014).

78. A. Villani, D. Malkin, U. Tabori, Syndromes predisposing to pediatric central nervous system tumors: lessons learned and new promises. *Current neurology and neuroscience reports* **12**, 153 (Apr, 2012).

79. P. Buczkowicz, U. Bartels, E. Bouffet, O. Becher, C. Hawkins, Histopathological spectrum of paediatric diffuse intrinsic pontine glioma: diagnostic and therapeutic implications. *Acta neuropathologica* **128**, 573 (Oct, 2014).